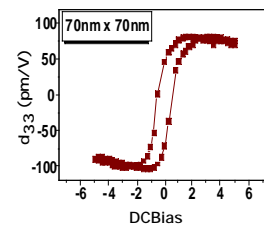
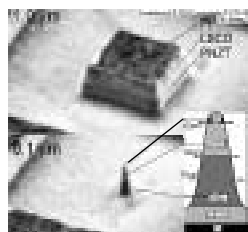


NANOSCALE PHENOMENA IN PEROVSKITE THIN FILMS



DOE Review FY2002

Participating Institutions



O. Auciello, J. A. Eastman,
G. B. Stephenson,
S. R. Phillipot, S. K. Streiffer



L. Boatner
R.A. McKee

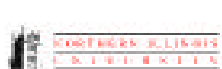


P. Clem, D. B. Dimos
B. G. Potter, B. A. Tuttle



M. Hawley

Northwestern



C. Thompson

UNC-Chapel Hill



M. J. Bedzyk
V. P. Dravid

Univ. Maryland



E. A. Irene



R. Ramesh



D. P. Norton

INDUSTRIAL ASSOCIATES

AGILENT

ATMI

IONWERKS

SYMETRIX

RADIANT

Vision

- Advance the science and technology of perovskite thin films for a new generation of microdevices and microelectro-mechanical systems (MEMS)
- Effectively couple existing National Laboratory / DOE-Basic Energy Science Programs on perovskite thin films, which are relevant to DOE's programmatic objectives for the 21st Century
- Perform research relevant to the Nanoscience / Nanotechnology National Initiative

Scope

● Basic science

- Basic science of crystalline perovskite film/semiconductor interfaces
- Basic science of established and novel piezoelectric thin films
- Nanoscale science and technology of perovskite thin films

● Enabling science for nanotechnologies

- Revolutionary gate oxides for next generation IC's
- Novel energy storage capacitors, ferroelectric memories and dielectric tunable microwave devices
- Novel MEMS technology

Impact

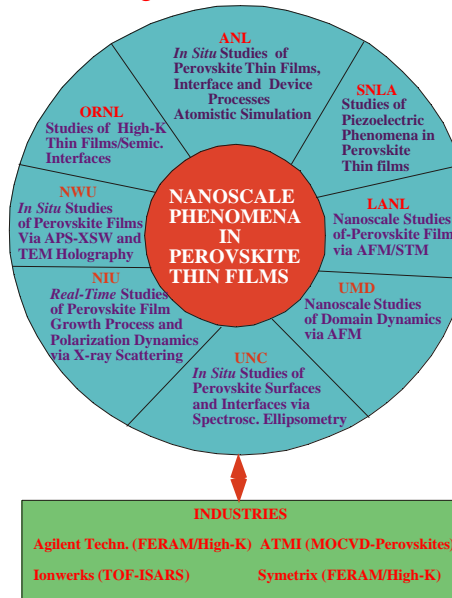
● New science

- Nanoscale structures and systems lead to new phenomena

● Novel nanotechnologies

- New materials
- Revolutionary concepts for device scaling
- New phenomena for new technologies

S&P Perovskite Project Team and Research Themes



Scientific Issues

- **Growth of perovskite films with precise control**
 - Chemical & microstructural
- **Control of compatibility for integration with dissimilar materials**
 - Interfacial interactions
 - Control of strain during processing and cooling
- **Nanoscale ferroelectric behavior**
 - Processing - microstructure - property relationships
 - Domain dynamics at the nanoscale

Task 1 - Studies of Perovskite Film Growth and Interface Processes

- **Studies of growth of key perovskite films**
 - $(\text{Ba},\text{Sr})\text{TiO}_3$, SrTiO_3 , PbTiO_3 , $\text{Pb}(\text{Zr},\text{Ti})\text{O}_3$, KNbO_3
- **Growth techniques**
 - MBE, MOCVD, Sputtering, PLD
- **In-situ evaluation of film growth and interface formation and processes**
 - RHEED (ORNL)
 - Studies of thin films growth process via *in situ* synchrotron X-ray scattering and standing wave (XSW) techniques at the APS (ANL, NIU, NWU)
 - Studies of Perovskite and barrier layers via TOF-ISARS/XPS/ spectroscopic ellipsometry (SE), TEM, and Electrical Characterization (ANL, UNC, ORNL)
- **Interface characterization: Z-contrast STEM (ORNL)**

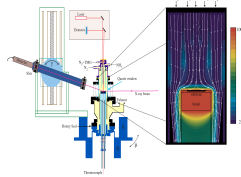
Task 2 - Nanoscale Structure- Property Relationships in Perovskite Systems

- **Evaluate influence of microstructure, strain, and interfacial chemistry on ferroelectric properties**
 - Control film variables (grain size, orientation, reactions) through fabrication (ANL, SNL, ORNL)
 - Determine effect of interfacial chemistry on Perovskite film properties (ANL, ORNL, UNC, NWU, UMD)
 - Studies of strain vs. perovskite film composition and substrate type (SNL)
 - Evaluation of superlattice heterostructures for controlling strain (ORNL, UF, ANL)

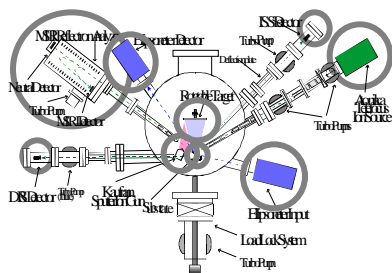
Task 2 - Nanoscale Structure- Property Relationships in Perovskite Systems - Cont.

- **Study ferroelectric and piezoelectric properties at the nanoscale**
 - Studies of ferroelectric domain at the nanoscale via AFM piezoresponse imaging (LANL, UMD, ANL)
 - Real-time X-ray synchrotron scattering and XSW for switching dynamics in ferroelectric thin films (ANL, NIU, SNL)
 - Nanoscale Studies of Charge Distribution and Current Transport in Perovskites Using Static and Dynamic TEM Electron Holography (NWU, ANL)
 - Molecular dynamics (ANL) and Monte-Carlo (SNL) simulations of phase transformation and ferroelectric domain motion and the influence of microstructure

MOCVD-oxide film growth system
at the BESSRC ANL-APS line for
studies of perovskite film growth
processes



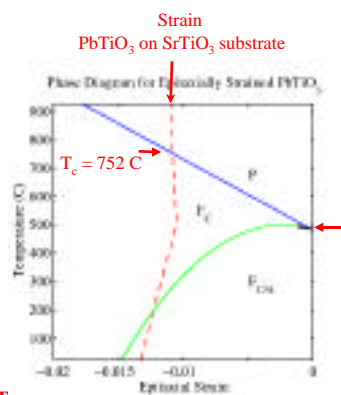
Task 1 - Studies of Perovskite Film Growth and Interface Processes



TOF-ISARS/Spectroscopic Ellipsometry
system at UNC-CH for film growth and
interface studies

Motivation for studies of PbTiO_3

- PbTiO_3 is a model ferroelectric material.
- High quality PbTiO_3 epitaxial thin films are produced by metal-organic chemical vapor deposition (MOCVD).
 - closely lattice matched to SrTiO_3 substrate
 - tetragonal axis normal to film on SrTiO_3 thin films can be grown
 - that are fully lattice matched (unrelaxed)
- Paraelectric-to-ferroelectric phase transition T_c predicted to depend on epitaxial strain.
 - 260°C enhancement predicted in T_c for PbTiO_3 on SrTiO_3



after N. A. Pertsev and V. G. Koukhar
PRL **84**, 3722 (2000).

G. B. Stephenson, J. A. Eastman,
S. K. Streiffer, O. Auciello,

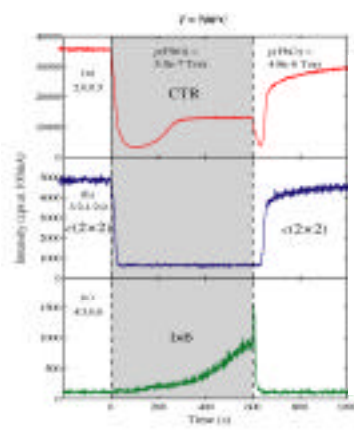
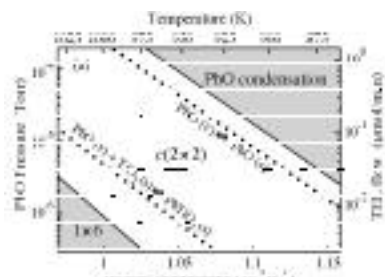
C. Thompson

Argonne

University of Chicago

PbTiO₃ Surface Structure

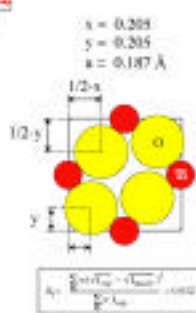
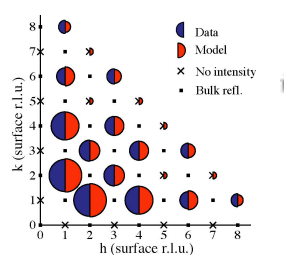
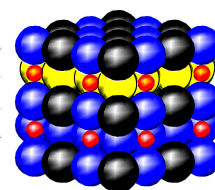
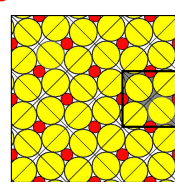
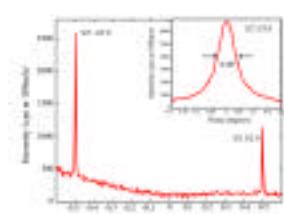
- A c(2×2) reconstruction is the equilibrium surface structure across the entire PbTiO₃ single-phase field.
- A poorly ordered (1×6) reconstruction is observed at PbO pressures below the PbTiO₃ stability line, and is believed to be a nonequilibrium Ti-rich structure.



A. Munkholm, S.K. Streiffer, M.V. Ramana Murty, J.A. Eastman, Carol Thompson, O. Auciello, J.F. Moore, and G.B. Stephenson, *Phys. Rev. Lett.* **88**, 016101 (2002).

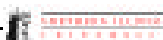


Model for PbTiO₃ $c(2 \times 2)$ Reconstruction



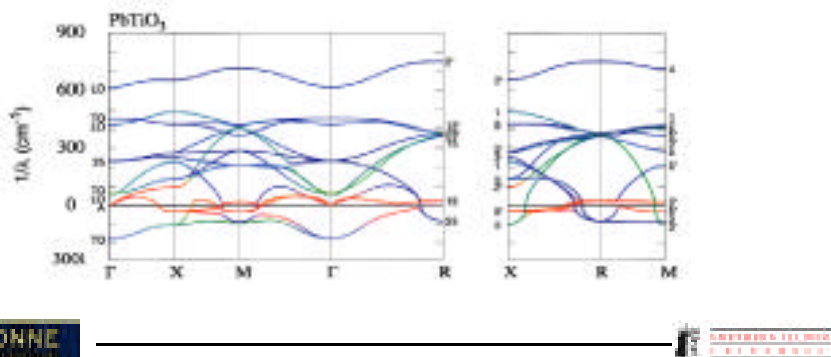
- Systematic absences imply four identical motifs per unit cell
- Small (2×2) R45° primitive unit cell greatly restricts plausible models

A. Munkholm, S.K. Streiffer, M.V. Ramana Murty, J.A. Eastman, Carol Thompson, O. Auciello, J.F. Moore, and G.B. Stephenson, *Phys. Rev. Lett.* **88**, 016101 (2002).



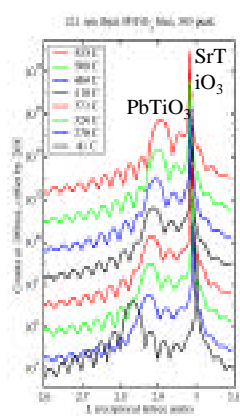
Surface Stabilizes Antiferrodistortive Mode

- Competing zone-center ferroelectric (yellow arrow) and zone-boundary antiferrodistortive (purple arrows) distortional modes have been identified by *ab-initio* calculations
 - W. Zhong and D. Vanderbilt, Phys. Rev. Lett. **74**, 2587 (1995).
 - Ph. Ghosez, E. Cockayne, U.V. Waghmare, and K.M. Rabe, Phys. Rev. B **60**, 836 (1999).
- Postulate that there is stabilization of the suppressed zone-boundary antiferrodistortive mode by the surface.

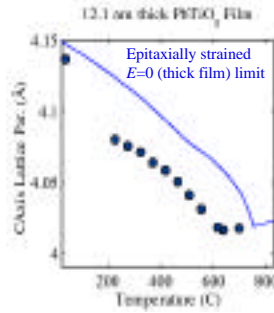


Argonne

Determination of T_c from c-axis lattice parameter

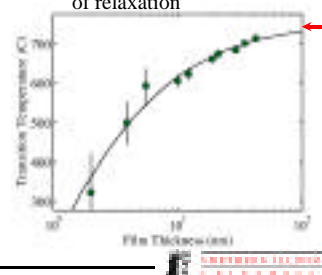


- Ferroelectric phase transition identified by measuring lattice parameter of PbTiO_3 as a function of temperature
- Phase transition is continuous T_c suppressed below $E=0$ LGD theory



Strong Variation of T_c with Film Thickness

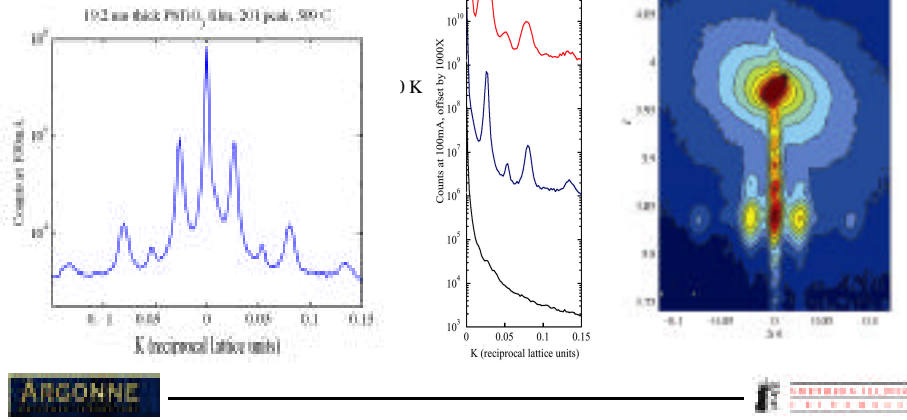
- T_c is suppressed with decreasing film thickness
- For thicker films, T_c approaches strained value, **752 C**, calculated by $E=0$ LGD theory
- Only PbTiO_3 films thinner than ~ 40 nm remain lattice matched to SrTiO_3
 - For thicknesses above 42 nm, irreversible relaxation occurs, T_c drops towards unstressed value depending upon amount of relaxation



Argonne

X-ray satellites observed \Rightarrow stripe domains

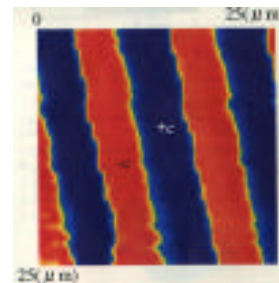
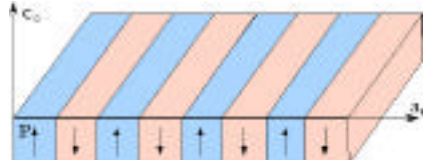
- Wavevector of modulation is in-plane
- Satellites with equal spacings in Q are observed at PbTiO_3 reflections with $L \neq 0$
- No satellites observed around $L=0$ peaks displacements are in c-axis direction



Argonne

Equilibrium 180° stripe domains in ferroelectrics

- Experimentally observed in bulk ferroelectrics (e.g., BaTiO_3), but no previous reports of their detection in thin films
- Associated with minimization of the depolarizing electrical field
- The presence of 180° stripe domains in thin films has been invoked to explain properties (e.g., Bratkovsky and Levanyuk, *PRL* 84, 3177, 2000 and *PRL* 85, 4614, 2000)

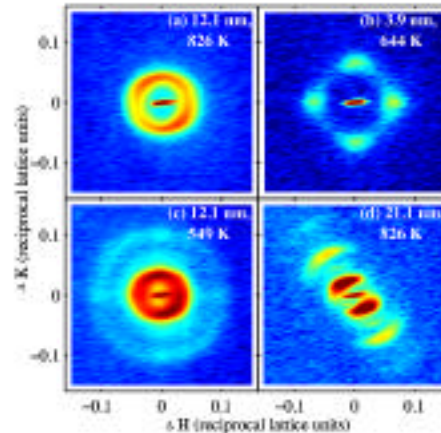


Y. Cho *et al.*, Jpn. J. Appl. Phys., **38**, 5689 (1999)

Argonne

180° stripe domain alignment varies from sample to sample

- Diffuse x-ray scattering patterns taken in $H-K$ plane through the PbTiO_3 304 peak show domain alignment
- Stripe domain alignments vary:
 - Thinner films (b) are typically aligned crystallographically
 - Some films (d) show stripes aligned to surface steps from substrate miscut
 - In other films (a,c), no preferred orientation occurs

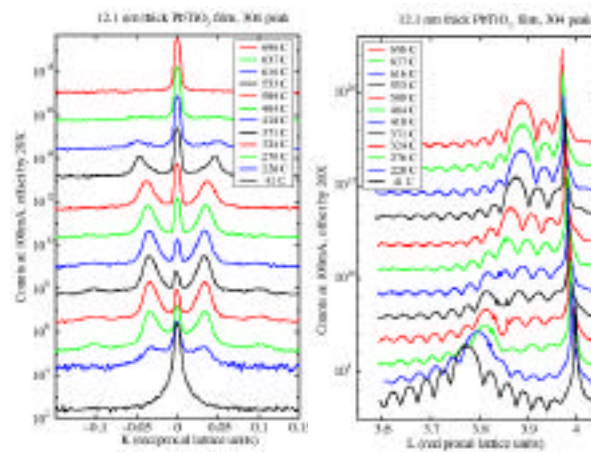


Argonne



Temperature dependence of x-ray satellites

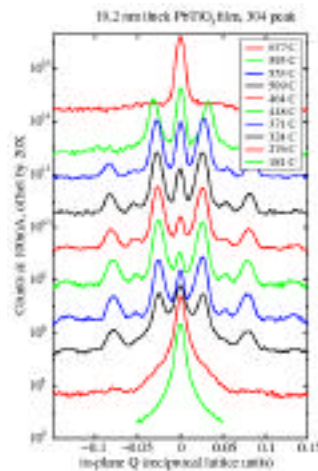
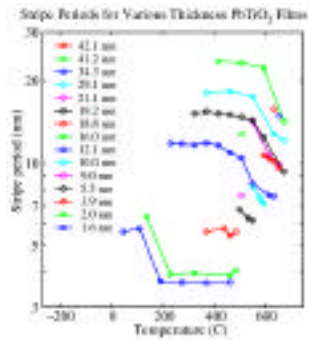
- Satellites appear at T_c
- Intensity of satellites increases with decreasing T
- Satellites disappear at low T
- Spacing of satellites shifts ~ 100 K below T_c



Argonne



Abrupt increase of stripe period occurs ~100 K below T_c



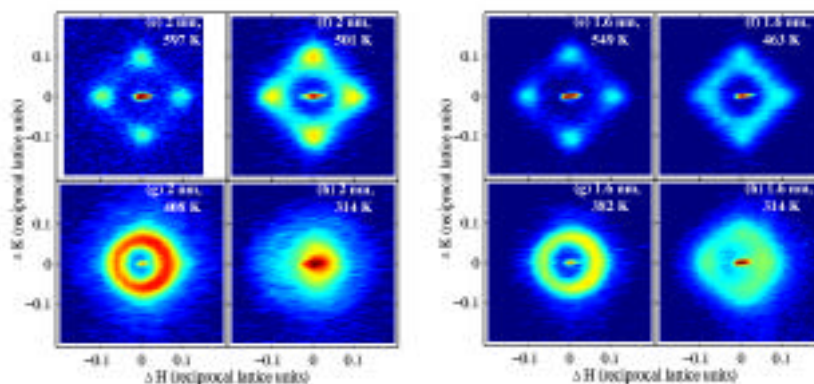
- Abrupt change of period is correlated with appearance of higher, odd-order satellites ($n = 3, 5, \dots$)
 - implies a change in polarization profile of domain walls

ARCONNE

卷之三

Stripe domains in ultra-thin PbTiO₃ films

We have observed stripe domains in films as thin as 1.6 nm, with a ferroelectric transition above room temperature



1.6 nm: $T_c = 580$ K

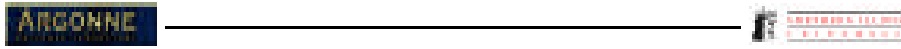
ARCONNE

卷之三

Theory for 180° Stripe Domains

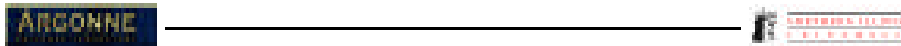
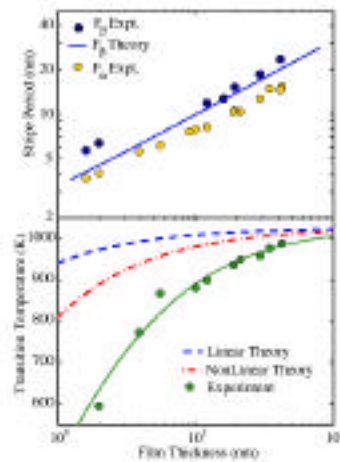


- 180° domain wall energy of 132 mJ/m² determined from ab-initio calculations (B. Meyer and David Vanderbilt, arXiv:cond-mat/0109257).
- All materials parameters are known, allowing comparison of theory and data with **no adjustable parameters**.



Comparison of stripe periods and T_c with theory

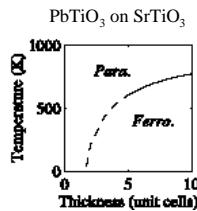
- Stripe domain period as a function of film thickness agrees with theory
- T_c is suppressed with decreasing film thickness, but **more** than predicted by models for stripe domain formation intrinsic surface effect may be important (A.G. Zembilgotov et al., *J. Appl. Phys.* **91**, 2247 (2002))



Nanoferroelectrics: Ultimate Size Limit



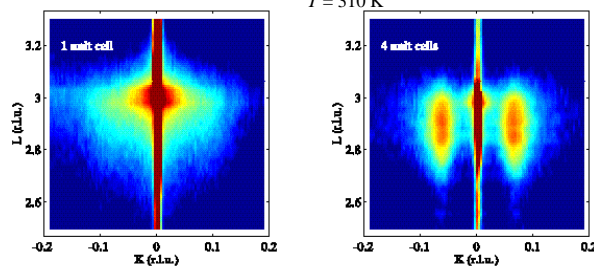
Diffuse X-ray scattering from 180° stripe domains identifies the ferroelectric phase



A strong size effect tends to suppress ferroelectricity in thin films.

We have grown extremely thin PbTiO_3 films showing a clear ferroelectric phase transition, stabilized by epitaxial strain.

What will be the ultimate size limit in nanostructures?



Argonne



Results: Equilibrium 180° stripe domain behavior

- 180° stripe domains appear at T_c during cooling
- Change in domain structure occurs $\sim 100 \text{ K}$ below T_c
- Finally, stripe domains disappear at lower temperatures
 - stripes would not appear in room temperature studies
 - consistent with previous findings of unidomain films
- Domain orientation can show several morphologies
- Systematic variation of stripe period and depression of T_c with film thickness
 - period agrees with theory (no adjustable parameters)
 - depression of T_c larger than expected solely from stripe domains

Argonne



Future work for x-ray studies of ferroelectric films

- Vary epitaxial strain conditions
 - study $\text{Pb}(\text{Zr},\text{Ti})\text{O}_3$ films
- Further studies on very thin films, down to single unit cells
- Use x-ray Bragg rod analysis to measure non-uniformity in the polarization distributions in very thin films
 - collaboration with Y. Yacoby, *et al.*
- We believe that the detailed structural information obtained by such x-ray studies will make further theoretical modelling very worthwhile

ARGONNE



IN-SITU, REAL TIME STUDIES OF INTERFACE FORMATION AND ELECTRICAL PROPERTIES OF BST THIN FILMS ON Si SUBSTRATES

- High K films on Si as MOSFET gate dielectric:
 - Binary oxides (ZrO_2 , HfO_2 ...)
 - Complex oxides ($\text{Ba}_x\text{Sr}_{1-x}\text{TiO}_3$, SrTiO_3 , BaTiO_3)
- Processing incompatibilities:
 - Elevated temperature and O_2 pressure required during deposition/processing of film
 - Interface formation & subcutaneous oxidation of Si

E. A. Irene



UNC-Chapel Hill

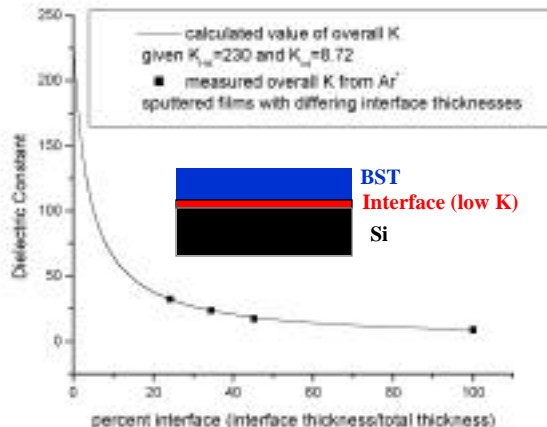
J.A. Schultz

IONWERKS

O. Auciello

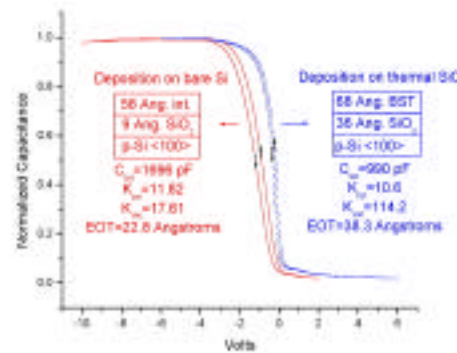
ARGONNE

Effect of low K layer

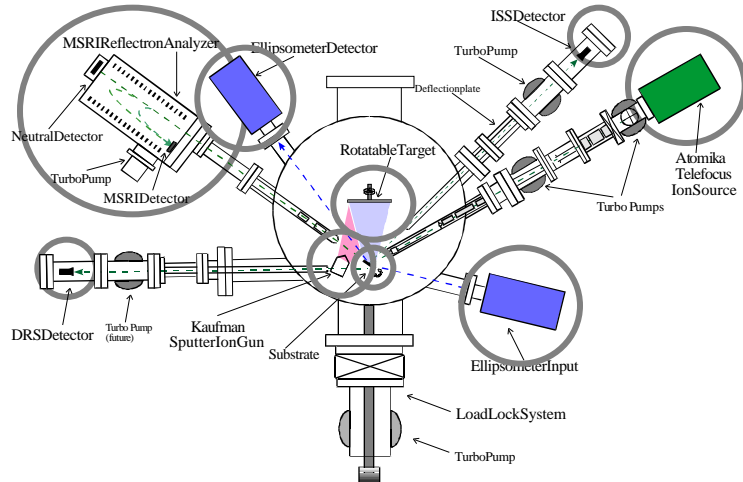


BST for MOSFET

- BST / Si interface
 - Degradation of K
 - Flatband shift
 - Hysteresis
 - Si surface states not passivated



TOF-ISARS/SECTROSCOPIC ELLIPSOMETRY SYSTEM



UNC-Chapel Hill

IONWERKS

ARGONNE
NATIONAL LABORATORY

Investigation of Interface Formation

- Real-time SE and MSRI studies of:
 - BST deposition on Si and SiO_2
 - Annealing in O_2 ambient

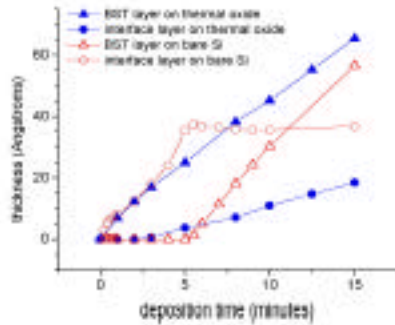
UNC-Chapel Hill

IONWERKS

ARGONNE
NATIONAL LABORATORY

Real Time SE: BST deposition on Si vs. SiO_2

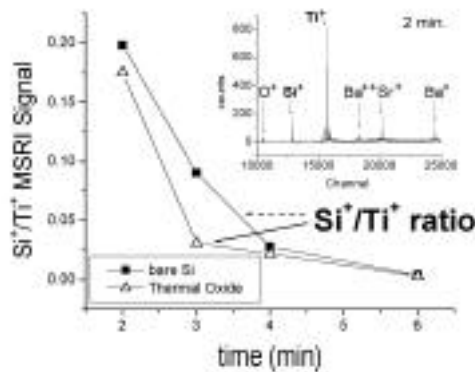
- BST deposition parameters:
 - Temp: 450°C
 - ion: Ar^+
- Si
 - Initial growth of interface (mixed) layer
 - BST growth begins after interface stops
- SiO_2
 - Initial growth pure BST phase
 - Interface forms slowly after some incubation time



UNC-Chapel Hill IONWERKS

ARGONNE

Real Time MSRI Study of BST/Si Interface Mixing

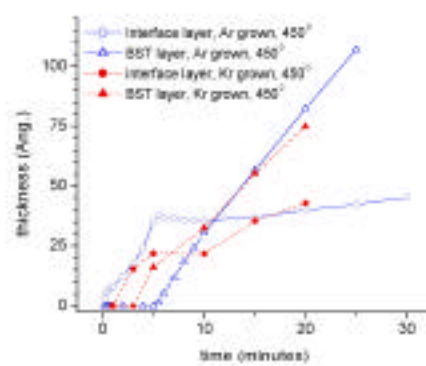


MSRI spectra taken during initial stages of BST growth show extent of intermixing greater for films grown on bare Si than thermal SiO_2

UNC-Chapel Hill IONWERKS

ARGONNE

Effect of Ions Scattered from Target on Growing BST Films



- Mass difference of ions results in different scattering cross-section
- Back-scattered Ar^+ ions have at least 2 effects
 - Si surface bombardment increases reactivity
 - Ion incorporation into film



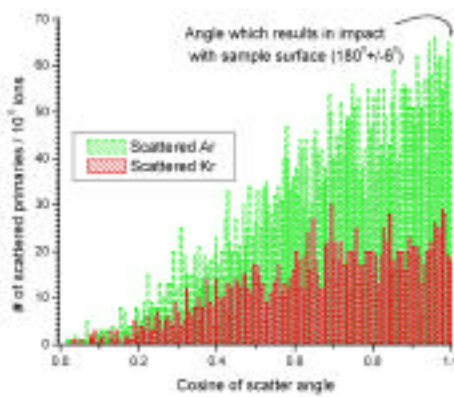
UNC-Chapel Hill

IONWERKS

ARGONNE

Calculated Spatial Distribution of Ions Scattered from Target that Impact on the Growing BST Films

- $\text{Ar} = 50/10^5$ ions
- $\text{Kr} = 18/10^5$ ions
- Sputter ion dose: 1.6×10^{17} ions/sec

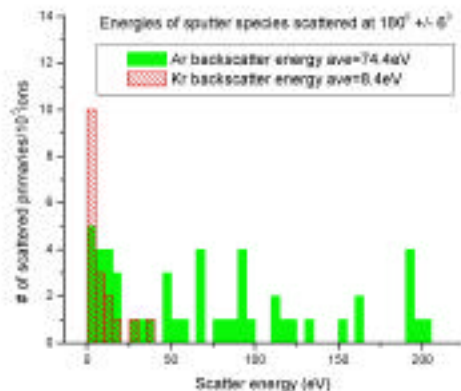


UNC-Chapel Hill

IONWERKS

ARGONNE

Calculated Energy Distribution of Ions Scattered from Target that Impact on the Growing BST Films



UNC-Chapel Hill

IONWERKS

ARGONNE

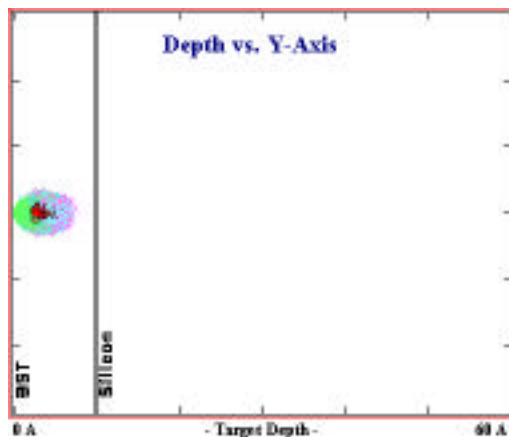
TRIM Calculation of Kr Ions Penetration Into BST

Effect of BS Kr on
10 Å BST on Si

Ion range: 3 Å

Collisions limited
to BST layer

- Sr/O
- Ba
- Ti
- Kr (moving)
- Kr (stopped)
- Si



UNC-Chapel Hill

IONWERKS

ARGONNE

TRIM Calculation of Kr Ions Penetration Into BST

Effect of BS Ar on
10Å BST on Si

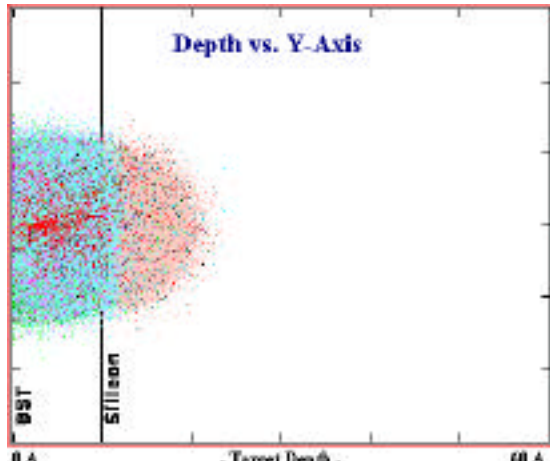
Ion range: 7Å

Significant impact
Beyond BST layer

- [■] Sr/O
- [■] Ba
- [■] Ti
- [■] Ar (moving)
- [■] Ar (stopped)
- [■] Si



UNC-Chapel Hill

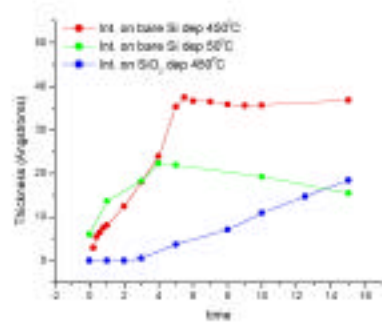


IONWERKS

ARGONNE

Si migration through BST film

- Deposition temperature is seen to increase the initial interface growth
- Interface thickness increases slowly with time for samples grown at elevated temperatures



UNC-Chapel Hill

IONWERKS

ARGONNE

Si migration through BST film

Layer	Pre-anneal thickness	Post anneal thickness
BST	64.2 Å	56.9 Å
Interface	10.8 Å	21.5 Å
SiO ₂	0 Å	15.8 Å

Table : SE model results pre and post
15 minute 650°C anneal in 1 mtorr O₂

- Annealing Studies suggest two Si migration mechanisms:
 - Fast: grain boundary- Si reaches surface, does not mix with BST
 - Slow: bulk diffusion- Si mixes with BST, extends interface thickness
- O migration and subcutaneous oxidation are also observed



UNC-Chapel Hill

IONWERKS



Summary

- Interface layer exhibits detrimental effects on overall dielectric film
- Interface formation is observed in real time
- Si diffusion and O migration observed
 - Reduction of SiO₂ by BST during anneal results in source of free Si

Future Work

- Studies of BST and STO growth and interface processes on ORNL template Sr-silicide layer on Si substrates



UNC-Chapel Hill

IONWERKS



***Silicide/Oxide Interfaces -
heteroepitaxy and its role in defining electrostatic boundary
conditions for the study of domain dynamics in ferroelectrics***

- Knowledge of path-dependent process and structure series for growing crystalline oxides on semiconductors (COS)
- Submonolayer silicides play a critical role in COS
- Studies of structure specific interface electrostatics:
 - Studies to understand how the silicide phases develop and how the transition from the silicide to the oxide occurs.

R. McKee, H. Hwang, K-Ju
F. Walker, M. Chisholm,
B. Shelton, M. Stocks



The MBE Laboratory

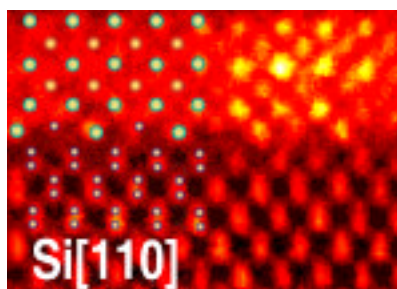
Duane Goodner
Mike Bedzyk



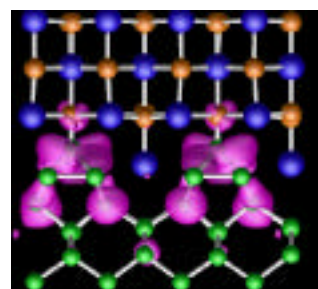
O. Auciello



***Interface Structure, Electrical Boundary Conditions
and Charge Transfer***



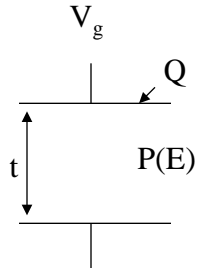
physical displacements at interface occur
in response to dipole electrostatic forces



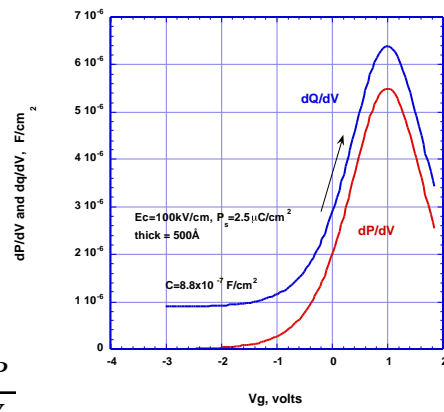
The MBE Laboratory



Polarization electrostatics - first case: metallic boundary conditions



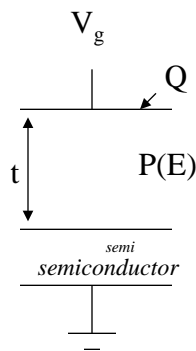
$$Q = CV_g + P \quad \frac{dQ}{dV_g} = C + \frac{dP}{dV_g}$$



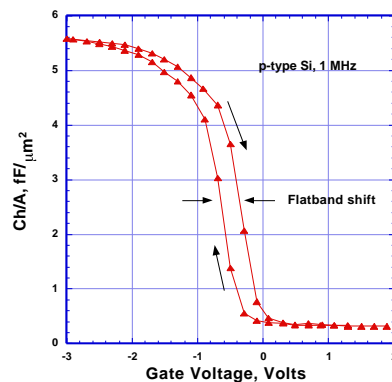
The MBE Laboratory



Polarization electrostatics - second case: semiconductor boundary conditions



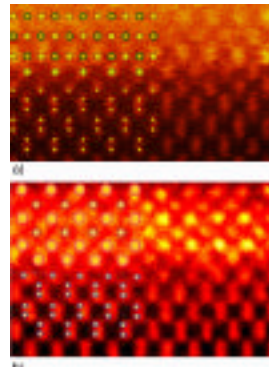
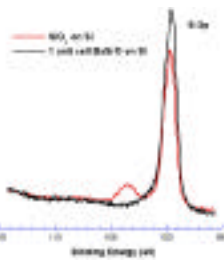
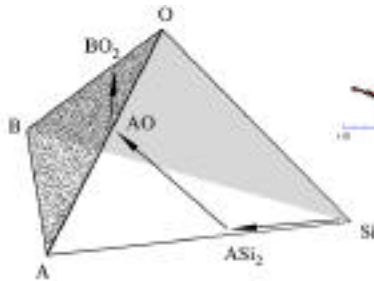
$$Q = C(V_g - \phi_{semi}) + P \quad \frac{dQ}{dV_g} = C + \frac{dP}{dV_g} - \frac{d\phi}{dV_g}$$



The MBE Laboratory



Oxide series: $(AO)_n(A'BO_3)_m$



Path-dependent stability to
avoid Si-containing oxides

Science **293**, 468(2001)



Bulk and surface structures of BaSi_2 on $(001)\text{Si}$

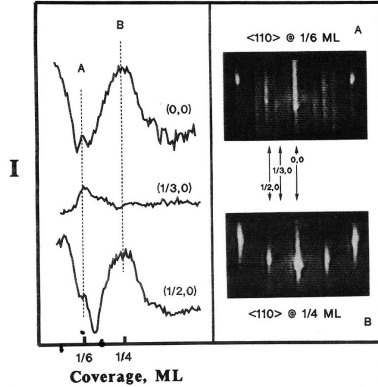
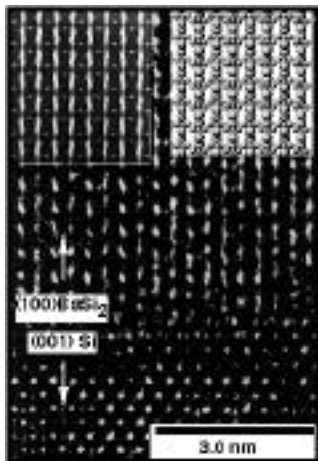
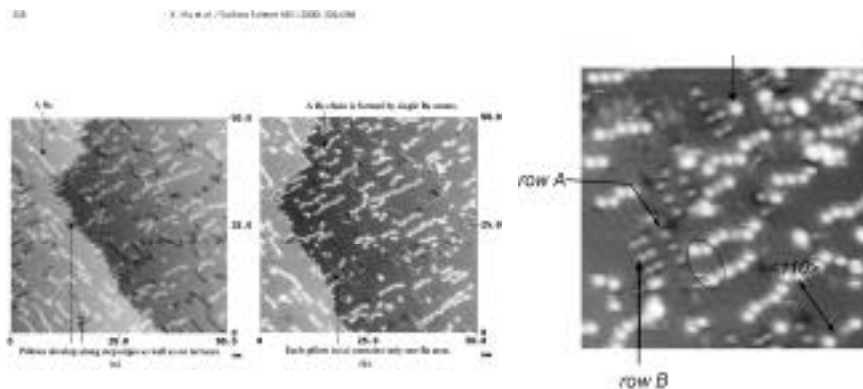


FIG. 5. Ordered surface RHEED patterns for submonolayer coverages.
Rod notation is based on surface unit mesh; zone axis is three-dimensional
convention.

Appl. Phys. Lett. **63**, 2818(1993)



Surface structure reports by Hu et al.



A two-phase mixture below 1/6ML-
What does it tell us?

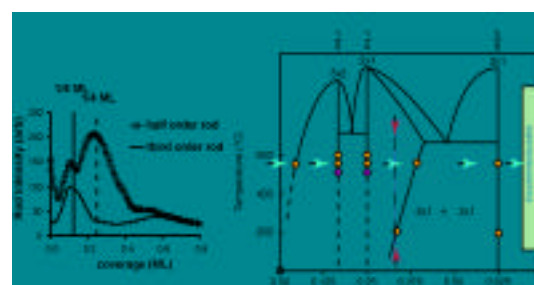


The MBE Laboratory



ARGONNE

Surface Structure and Phases for submonolayer silicides

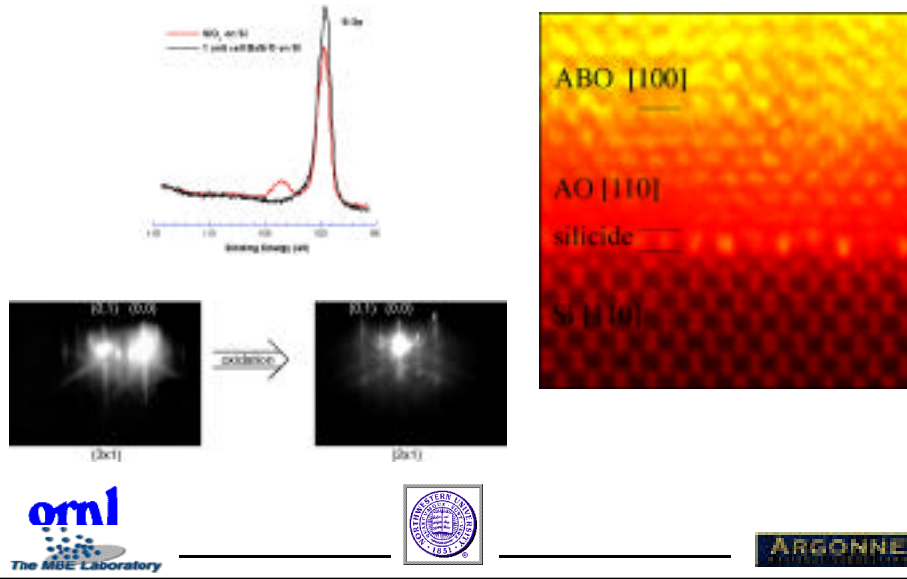


The MBE Laboratory

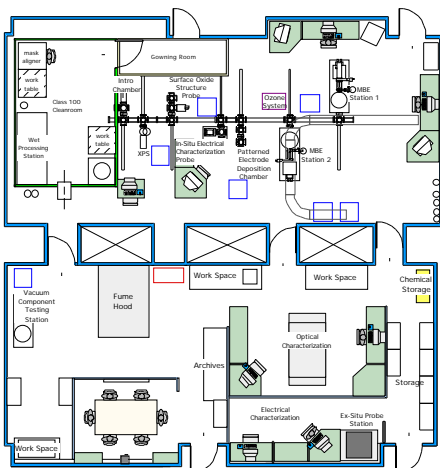


ARGONNE

The silicide is left behind to play a vital role in oxide interface electrical structure



The Future at the MBE Laboratory in ORNL



- 3000 ft² total space;
- 175 ft² of class 100 clean room
- 1/4 um feature size
- Mask aligner
- 2 MBE machines
- XPS
- In-situ probe station
- Ex-situ probe station
- Ozone processing
- Optical table

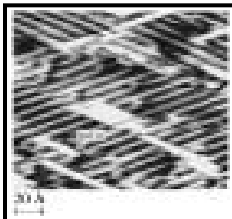
Total capital - \$2.7M



X-ray standing wave investigation of sub-monolayer Sr / Si(001) surface phases

Introduction

- Goal: Characterize atomic-scale structure of sub-monolayer Sr / Si(001) surface phases.
- Motivation: Alkali-earth metals on semiconductor surfaces is an important precursor to growth of perovskites on semiconductors. With a much higher dielectric constant, perovskites, such as SrTiO₃, are promising candidates for replacing SiO₂ as the gate-dielectric in FETs.



- LEED studies show several phases of Sr adsorbed on Si(001): (3 x 1), (5 x 1), (2 x 1), (3 x 2)
- STM investigation of (3 x 2) surface suggests Sr sits at cave site
- Debate over whether (3 x 2) phase has one or two Sr atoms per unit cell

0.3 ML(3 x 2) Sr/Si(001)
STM image

R. McKee, H. Hwang, K-Ju
F. Walker, M. Chisholm,
B. Shelton, M. Stocks



The MBE Laboratory

Duane Goodner
Mike Bedzyk

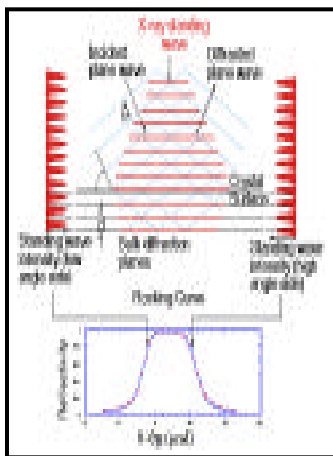


O. Auciello



X-ray standing wave investigation of sub-monolayer Sr / Si(001) surface phases

XSW Concept



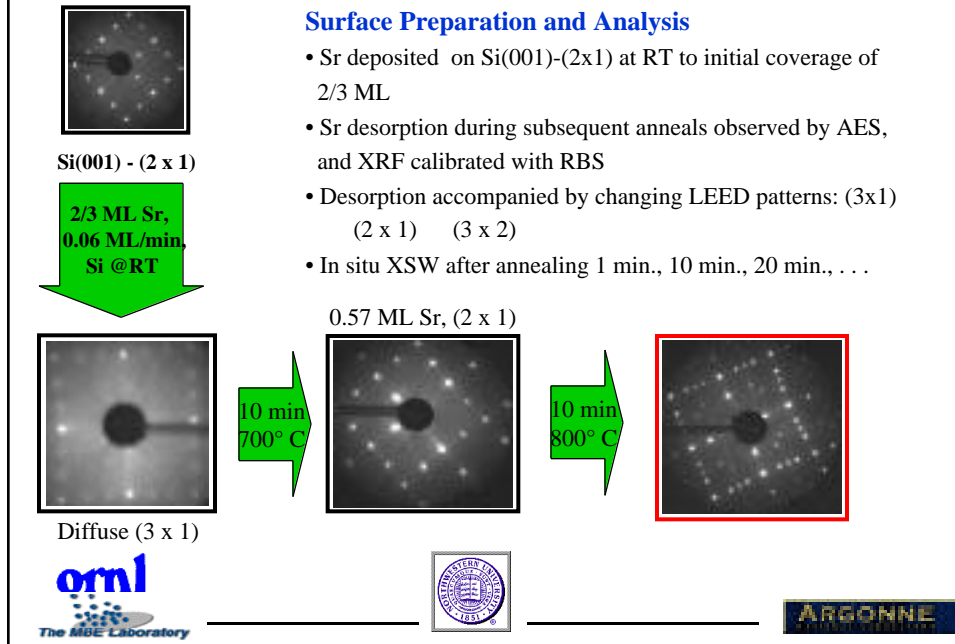
- Interference between incident and diffracted x-ray beam at bulk Si Bragg peak produces x-ray standing wave (XSW) of same periodicity (d) as bulk diffraction planes
- Scanning through rocking curve causes standing wave phase shift of $d/2$
- Corresponding modulation of Sr fluorescence (due to photoelectric effect) used to determine coherent fraction (f) and position (P) of adsorbate atoms from dynamical diffraction equation for fluorescence yield (Y):
- Off-normal Bragg reflection XSW analysis used to triangulate Sr position.



The MBE Laboratory

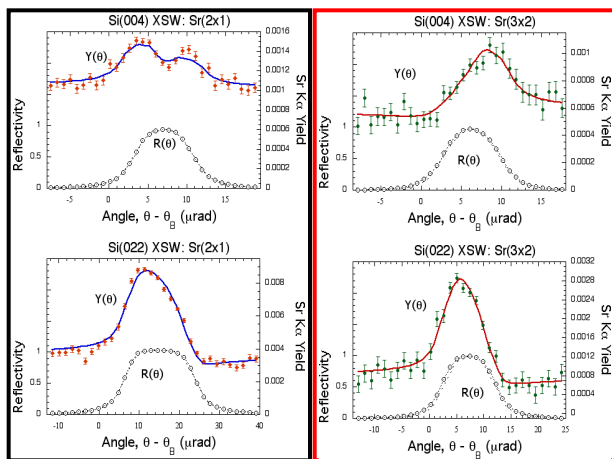


X-ray standing wave investigation of sub-monolayer Sr / Si(001) surface phases



X-ray standing wave investigation of sub-monolayer Sr / Si(001) surface phases

Experimental DATA



X-ray standing wave investigation of sub-monolayer Sr / Si(001) surface phases

XSW Results

LEED	P ₀₀₄	f ₀₀₄	P ₀₂₂	f ₀₂₂
(2 x 1) ^a	0.73 ± 0.01	0.42 ± 0.01	0.34 ± 0.01	0.89 ± 0.02
(3 x 2) ^b	0.89 ± 0.01	0.37 ± 0.03	0.39 ± 0.01	0.64 ± 0.07

a = 10 min 750° C

b = 10 min 750° C + 10 min 800° C

Symmetry rule for cave or bridge site occupation:

$$P_{022} = \frac{P_{004}}{2}$$

- Good agreement for (2 x 1)
- (3 x 2) deviates from symmetry rule by 12%

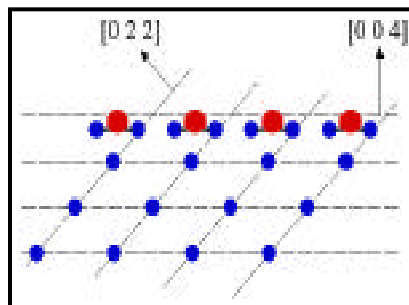


X-ray standing wave investigation of sub-monolayer Sr / Si(001) surface phases

XSW Interpretation

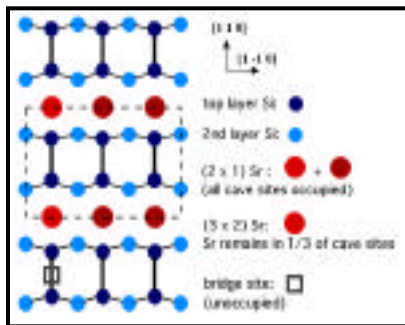
- Normal (004) and off-normal (022) coherent positions used to triangulate Sr position
- P₀₀₄ and P₀₂₂ values satisfy symmetry rules for both cave and bridge sites, but intact Si dimers observed by STM suggests bridge site is unoccupied

Side view: [-100] projection of dimerized Si(001) surface with Sr (●) atoms at cave site



X-ray standing wave investigation of sub-monolayer Sr / Si(001) surface phases

Surface Model for (2 x 1) and (3 x 2) phases



Conclusions

- Sr adsorbed at cave site in (2 x 1) and (3 x 2) phases (as previously suggested by STM)
- (3 x 2) phase has 1 atom per unit cell, contrary to early STM study, but in agreement with recent results⁵
- XSW indicates Sr located 1.00 Å above bulk extrapolated Si(004) plane and 0.65 Å outward from Si(022) planes
- 12% deviation from cave site symmetry rule exhibited by 0.15 ML (3 x 2) may be due to secondary site occupation

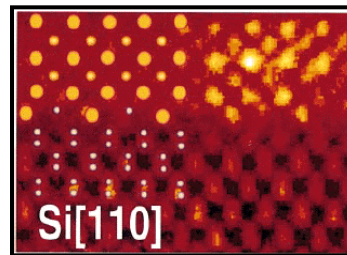


X-ray standing wave investigation of sub-monolayer Sr / Si(001) surface phases

Future Work

XSW, XAFS, and SXRD studies of:

- Adsorbed phases of Ba on Si and Ba on Ge
- 1/4 ML alkali-metal silicide c(4 x 2) surface phases used as templates for growth of crystalline oxides on semiconductors (COS)
- Atomic-scale structure of COS interfaces



Z - contrast TEM of SrTiO₃ grown on c(4 x 2) Sr/Si(001) template layer¹



Task 2 - Nanoscale Structure- Property Relationships in Perovskite Systems

Stress-Induced Orientation and Impact on Piezoelectric and Dielectric Properties of PZT Thin Films

Multi-Organizational Effort Searches for Nanostructural
Origins of Macroscopic Properties

PZT films fabricated by MOCVD (ANL) and CSD (SNL)
permits wide range of structural evolution

- Single crystal to fine grain mono- 90° domain polycrystalline materials
- 100% a-domain PZT films possible with UMD (100) SrTiO₃ on Si substrates
- KTaO₃ single crystals (ORNL) Provides excellent Lattice match for growth template and Compressive stress favors c-domains (low number density of a/c domain walls)
- AFM (LANL and UMD) to characterize growth and piezoelectric response
- FIB to determine size - domain effects on ferroelectricity

B. Tuttle, P. Clem, J. Dawley,
G. Brennecke, D. Williams,
J. Wheeler, W. Olson, and
M. Bourbina



S. Streiffer,
O. Auceillo,
G. Bai



R. Ramesh,
N. Naoloan
L. Boatner

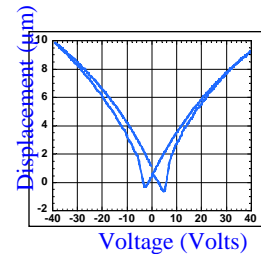


M. Hawley



SNL/ANL Collaboration: Impact of Nanoscale Genesis of Domains on Piezoelectric Response

- Domain Orientation Influence on Piezo-response
- Films: ANL MOCVD, SNL CSD
- Crystallinity: Random Polycrystalline ensembles to Oriented Single Crystal
- SNL Supplied Thin Si and Highly 001 Oriented Pt / MgO Substrates to ANL
- SNL Characterized Piezo Response of CSD PZT on Pt coated MgO and Si Wafers



SNL CSD PZT Film on Thin Si



Cantilever Beams With Different Molecular Sensitivities



Sandia National Laboratories



ARGONNE
NATIONAL LABORATORY



ORNL



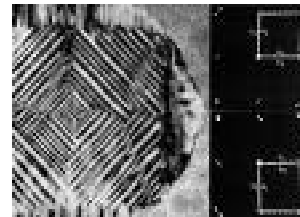
Los Alamos
NATIONAL LABORATORIES

LANL, RTI, SNL Collaboration to Develop Fundamental Understanding of Nano-Level Response of PZT Films

Atomic Force Microscope

Compliant beam bends when attracted to surface.

Piezo-response Measured at Nanoscale Level By AFM



Domain Structure: PZT 40/60 // MgO

B. Tuttle



Sandia National Laboratories

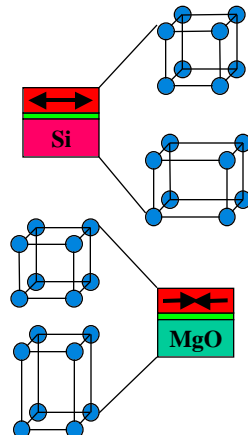
J. T. Evans
Radiant

M. Hawley



Transformation Stress Concept* Based on Three Postulations

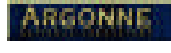
- Mechanical stress state of film during cooling through Curie temperature determines 90° domain orientations
- Electrical switching of 90° domains is very limited in tetragonal thin films
- Mono-90° domain grains accentuate property differences



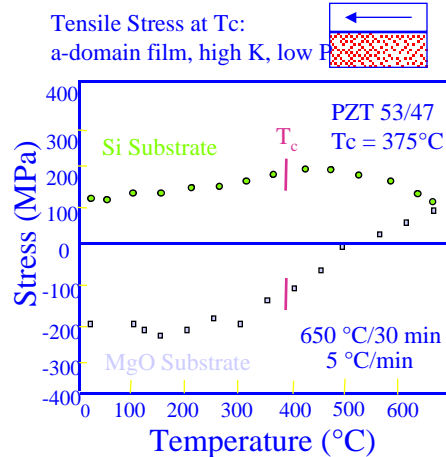
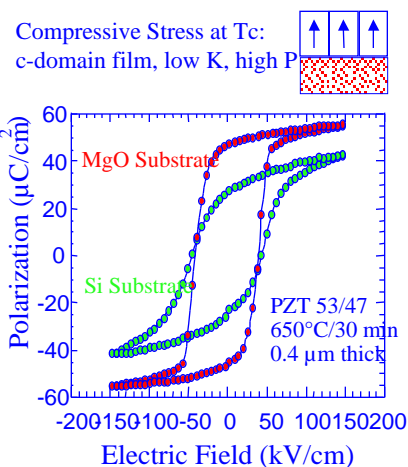
*Tuttle et.al., Ferroelectrics, Vol.221, 209-18 (1999)



Sandia National Laboratories



Domain structure of ferroelectric films is determined by film stress at the Curie temperature



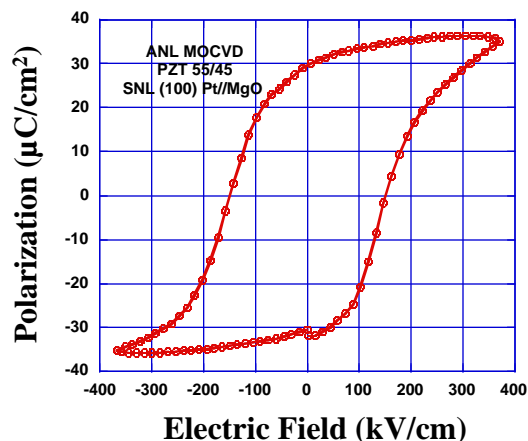
Sandia National Laboratories



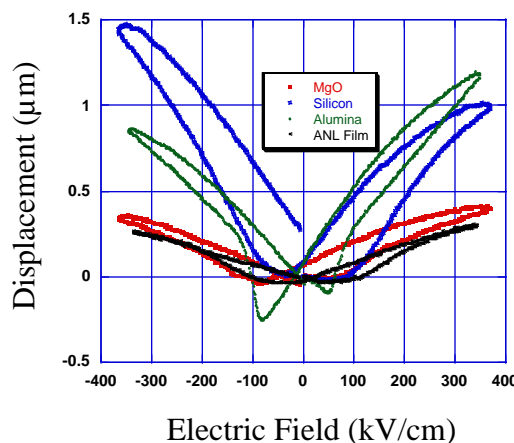
ANL MOCVD Film Exhibits Good Dielectric Hysteresis

ANL MOCVD
PZT 55/45
0.85 μm thick
 $F = 1\text{kHz}$

SNL
(100) Pt //
MgO



Displacement vs. Field Behavior of PZT 40/60 Films on Different Pt Coated Substrates

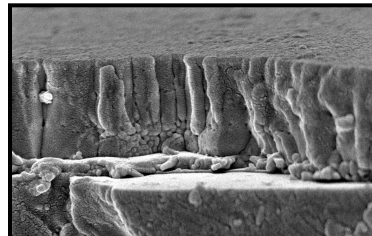


ANL MOCVD
PZT 55/45
Pt//MgO;

SNL CSD
PZT 40/60
Pt// MgO
Pt// Al_2O_3
Pt//Ti//Si

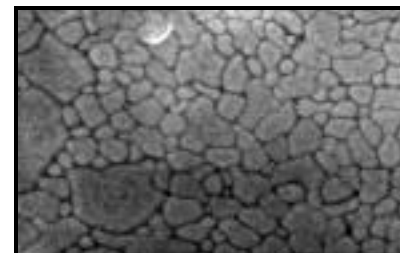


Displacement vs. Field Behavior of PZT 40/60 Films on Different Pt Coated Substrates



- Cross-section of PZT on Al_2O_3
- Columnar morphology
- Distinct Ti adhesion layer visible

- Plan view of PZT on MgO
- Most grains are $\sim 100\text{nm}$ or smaller

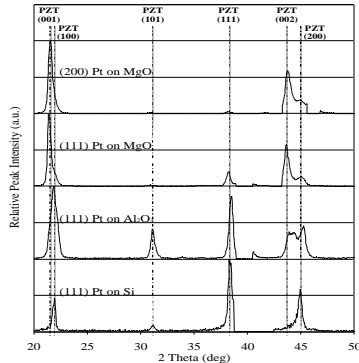
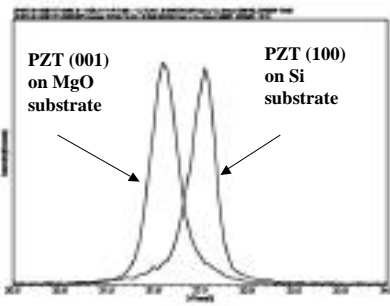


ARGONNE



Los Alamos
NATIONAL LABORATORIES

Stress Determines 90° Orientations



Substrate	Si	Al_2O_3	MgO	PZT
~ CTE (ppm/C)	4	9	13	7

Films are single phase perovskite
(Substrate and electrode
peaks have been removed)



ARGONNE

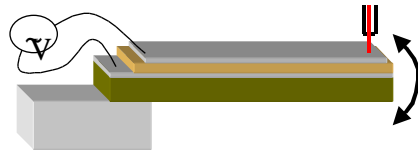


ornl

Los Alamos
NATIONAL LABORATORIES

Samples Tested as Cantilever Beams

- Top electrode is 1.5mm x 10mm shadow-masked Pt
- Beams diced with wafer saw
- Displacement measured with MTI Fotonic Sensor



$$d_{31} = \frac{S_{\max}}{3E} \quad \frac{1}{L^2} \quad \frac{t_{\text{sub}}^2}{t_{\text{film}}} \quad \frac{Y_{\text{sub}}}{Y_{\text{film}}}$$

	Si (100)	Al ₂ O ₃ (r-cut)	MgO (100)	PZT (40/60)
Modulus (GPa)	130	360	320	100
Thickness (μm)	330	330	500	0.6 - 1.0



Sandia National Laboratories

ARGONNE
NATIONAL LABORATORY

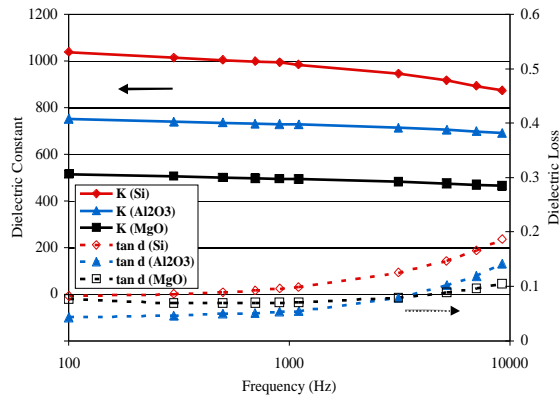


ornl

Los Alamos
NATIONAL LABORATORIES

Dielectric Constant Decreases with Increased c-axis Orientation

- Automated Sweep ($C_p, \tan \delta$)
- Frequency (100 Hz - 1 MHz)
- AC Voltage (100 mV - 10 V)
- DC Bias (0 V - 10 V)
- Measurements made prior to FE/PE tests



Sandia National Laboratories

ARGONNE
NATIONAL LABORATORY

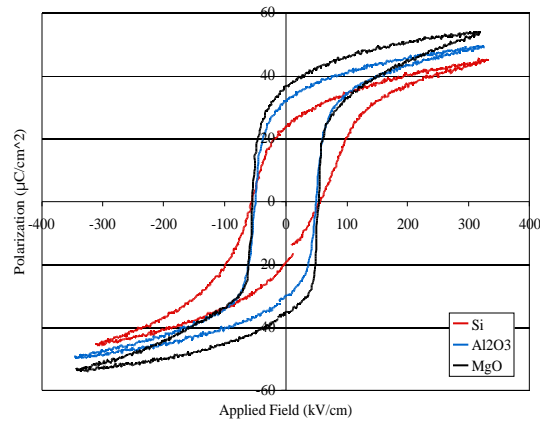


ornl

Los Alamos
NATIONAL LABORATORIES

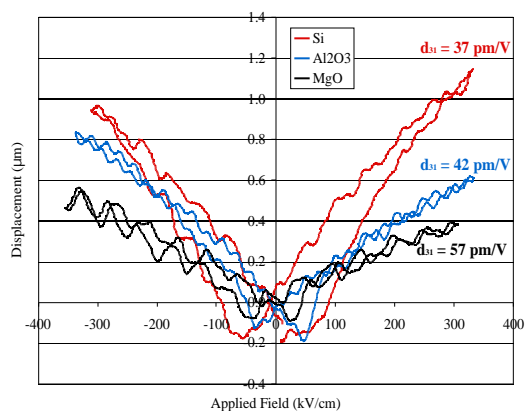
Remanent Polarization Increases with c-axis Orientation

- Tested at
- 375 kV/cm
- 1 kHz
- Coercive Field does not change with stress state
- Films tested up to 1MV/cm
- SNL CSD PZT 40/60 Films



d_{31} Increases with c-axis Orientation

- Tested at
- 375 kV/cm
- 1 kHz
- Substrate thicknesses
- Si: 330 μm
- Al₂O₃: 330 μm
- MgO: 500 μm
- Fluctuations are 60Hz noise



Oriented Film Properties Compared to Intrinsic Calculations

Substrate	Volume Fraction (100) (111) (001)	+Pr ($\mu\text{C}/\text{cm}^2$)		Dielectric Constant		d_{31}	
		Measured	Predicted Intrinsic	Measured	Predicted Intrinsic	Measured	Predicted Intrinsic
Si	27:73:0	22.4 +/- 1.6	27.4	983 +/- 21	405	37.3 +/- 3.2	24.9
Al ₂ O ₃	38:20:42	28.9 +/- 0.8	34.8	710 +/- 27	347	41.6 +/- 6.1	31.6
MgO	0:6:94	32.5 +/- 2.4	63.4	506 +/- 15	208	57.2 +/- 3.8	57.5

180° Domain Extrinsic Contributions Result in Jigher K than first order approximation

Haun, Cross; $K_{11} = 498$, $K_{33} = 197$
 $P_3 = 0.57$; $d_{33} = 162$, $d_{31} = -59$, $d_{15} = 169$
 Uchino,JJAP (1997)



Summary of Dielectric and Piezoelectric Data

	On Alumina	On MgO	On Silicon	ANL
P Max	34	25.6	21	35
Premanent	20.4	13.6	6.4	30
K	396	243	784	748
d31	42	57	37	36

Dielectric Constant (K) taken at 1 kHz and 0.1 Volt ac
 ANL Film is MOCVD 0.85 microns, PZT 55/45

Deposited on (100) Pt // MgO

All other films are SNLCSD 0.75 microns, PZT 40/60



Conclusions

- 90° domain structure can be tailored by controlling the stress state of the film during cooling through the Curie Temperature
- Properties of stress-oriented films follow trends predicted by single crystal calculations
- More work needs to be done to determine how nano-level interface phenomena controls the polarization - piezoelectric constant relationships



Sandia National Laboratories



Overcoming Suppressed Permittivity in (Ba,Sr)TiO₃

Fine grain size BaTiO₃ and BST thin films display suppressed ferroelectric behavior (CSD, MOCVD, and sputtered):

- suppressed K' (200-300)
- paraelectric/suppressed P_r
- absence of Curie-Weiss behavior

Several recent models have been developed for this:

Zhou/Newns

interfacial capacitance

Frey/Payne

low K' interface, [OH]

Pertsev/Tagantsev

strain effects on Dev/Landau

Streiffer/Basceri/Kingon

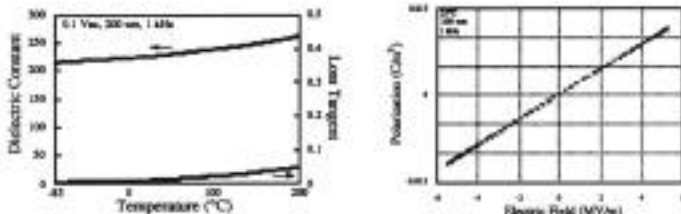
strain/interface/excess Ti

Do these models apply better to specific systems, than universally?

P. Clem



Nano- and polycrystalline CSD BaTiO₃ Thin Films



25nm grain size BaTiO₃, 0.2μm thick, 700C: paraelectric and cubic.

Grain size dependence: $K' = 230$ (25nm)

$K' = 270$ (40nm)

$K' = 310$ (50nm)[Frey/Payne]



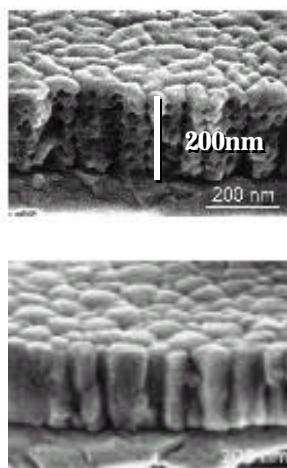
TEM indicates growth twins,
but not FE domains (stable to 500°C)



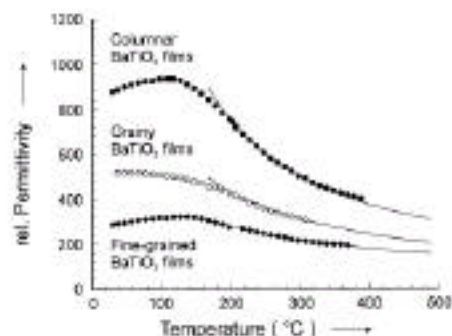
Sandia National Laboratories

Columnar vs. polycrystalline CSD BaTiO₃ Films

[Hoffman/Waser]



40nm polycrystalline film \rightarrow PE
60-100nm columnar films \rightarrow FE

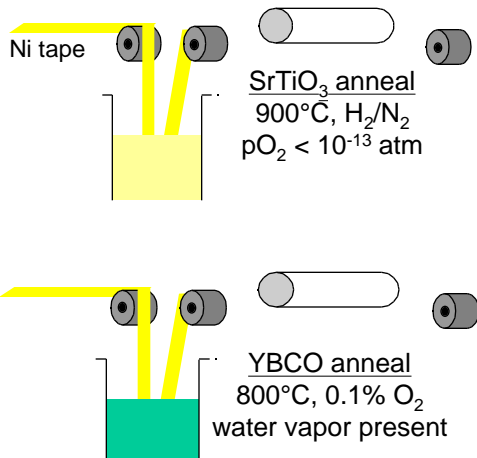


Temperature dependence of the permittivity of CSD-prepared BaTiO₃ thin films (thickness approx. 200 nm) as a function of the film morphology. The measurements were performed on Pt/BaTiO₃/Pt structures at 10 kHz with a 0.1 V signal.



Sandia National Laboratories

All Solution Deposition Schematic



Solutions are:
metal acetates
metal alkoxides
trifluoroacetic acid
solvents

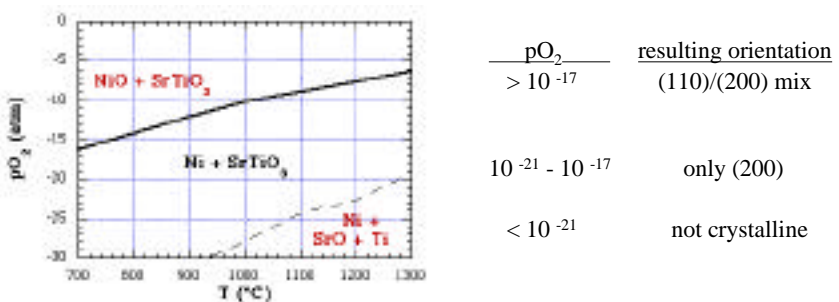
Coating parameters:
1-5 cm/s pull speed
0.1-0.4 $\mu\text{m}/\text{coating}$
 $J_c = 1.3 \text{ MA/cm}^2$
multilayering YBCO
(3-6 layers $> 1\mu\text{m}$)



Sandia National Laboratories

Ni oxidation limits pO_2 process regime

Ellingham plots of Ni and STO stability Buffer layer results



Consistent pO_2 values may be achieved with $\sim 0.1\% \text{ H}_2/\text{N}_2$.



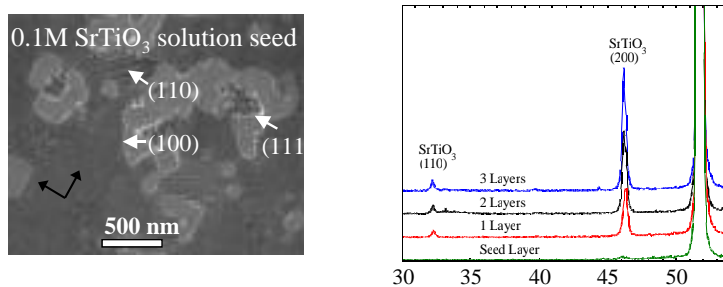
Sandia National Laboratories

Lattice mismatch, seeding of SrTiO₃

SrTiO₃ has a 10% lattice mismatch with Ni, which complicates epitaxy.

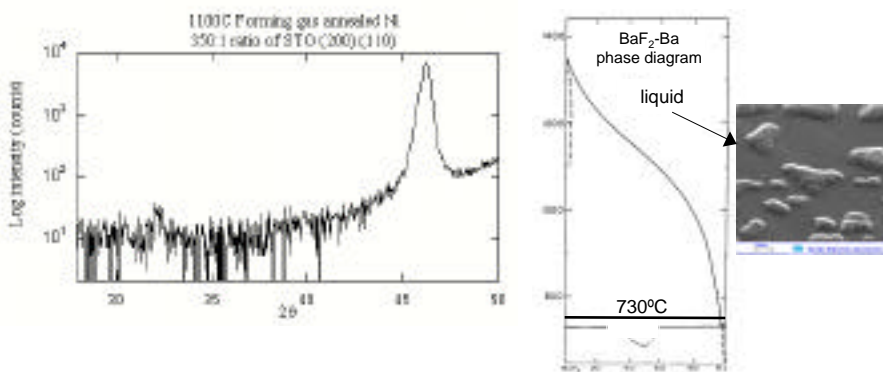
Seeded growth of SrTiO₃ and BaTiO₃ improves film nucleation, orientation.
[Schwartz, Clem, *et al.* J. Am. Ceram. Soc. 82(9) 2359 (1999)].

- On Ni(200), lack of seeding results in randomly oriented SrTiO₃ films
- Random (110) components of STO YBCO (103) later

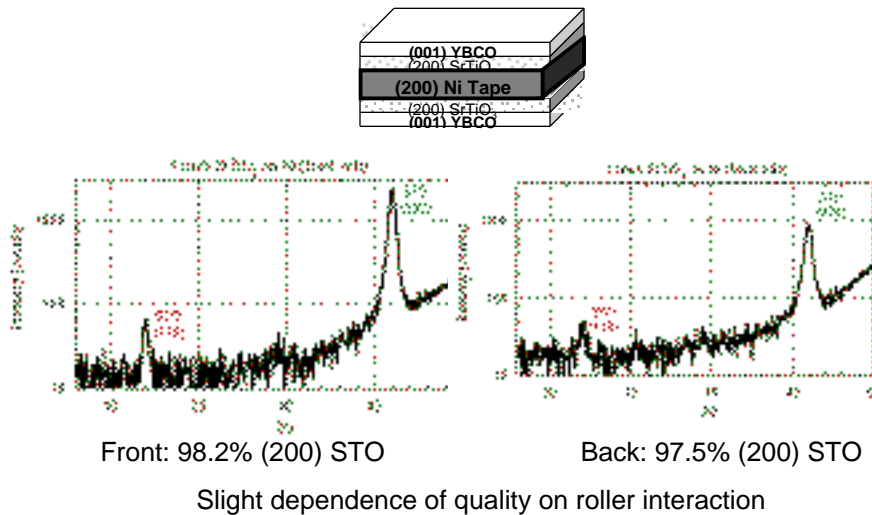


Halide precursors enhance epitaxy of alkaline earth oxides

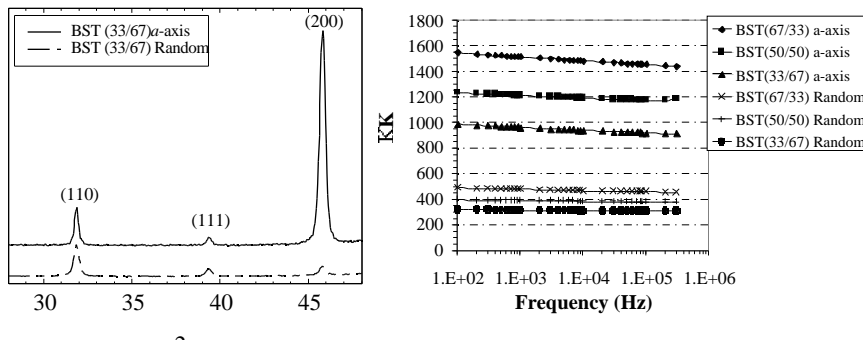
Using a fluorinated solution approach similar to that for sol-gel YBCO, other oxides, such as BaTiO₃ and SrTiO₃, show enhanced orientation.
(US Patent 6,231,666, Clem et al., 2001)



Halide precursors enhance epitaxy of alkaline earth oxides



(100) oriented, columnar BST displays enhanced permittivity on Ni substrates



Over a threefold improvement in permittivity (K' up to 1500) for BST on base metal Ni substrates due to oxidation control and columnar (100) growth.

Loss $\tan \delta = 0.003$ to 0.015 for $\text{Ba}_x\text{Sr}_{1-x}\text{TiO}_3$ ($x = 0$ to 0.67)



Future Work: Address remaining questions for ferroelectric suppression in BaTiO₃

Is there a common FE critical size (< 40nm)? Raman, XAFS, SHG

Do chemical defects (OH, C) play similar roles for CSD and CVD?

Do recent models apply well to thicker (> 100nm) FE films?

What are differences/similarities in FE suppression for MOCVD, sol-gel, MBE, and PLD methods; is columnar growth key for all?

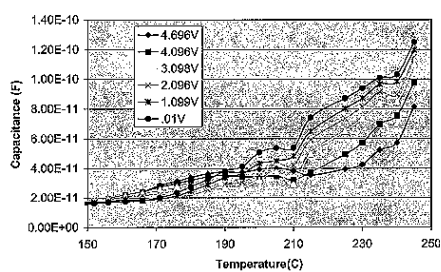
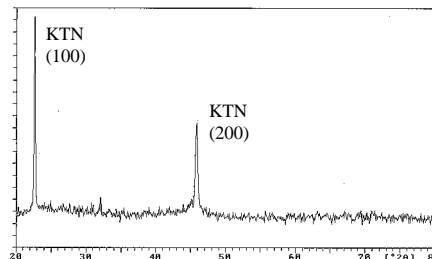
Analysis:

Synchrotron- lattice structure, orientation, domain formation
Raman- local structural symmetry
FE, electrical analysis: macroscopic behavior



Properties of KTaO₃/KNbO₃ Superlattices

- Effects of reduced dimensionality on ferroelectricity and phase transitions in the K(Ta,Nb)O₃ system



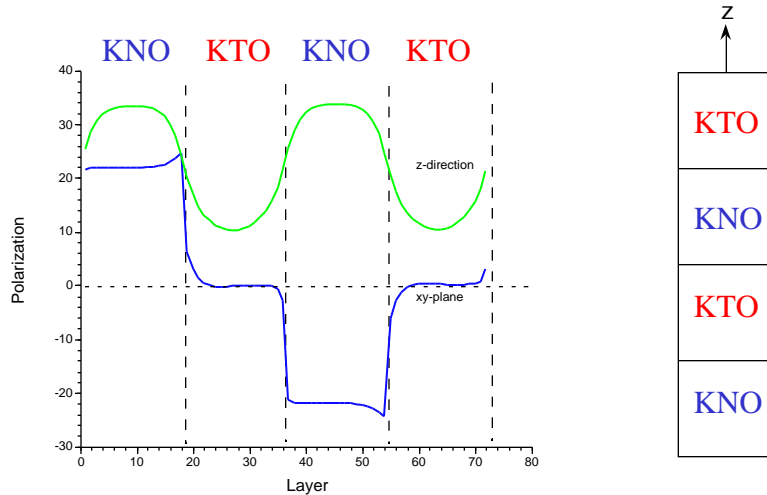
- Present: temperature-dependent dielectric properties of superlattices grown by pulsed-laser deposition
- Future: understanding the atomic layer-by-layer growth mechanisms for the formation of 1-D wire-like structures

D.P Norton



L. Boatner
ornl

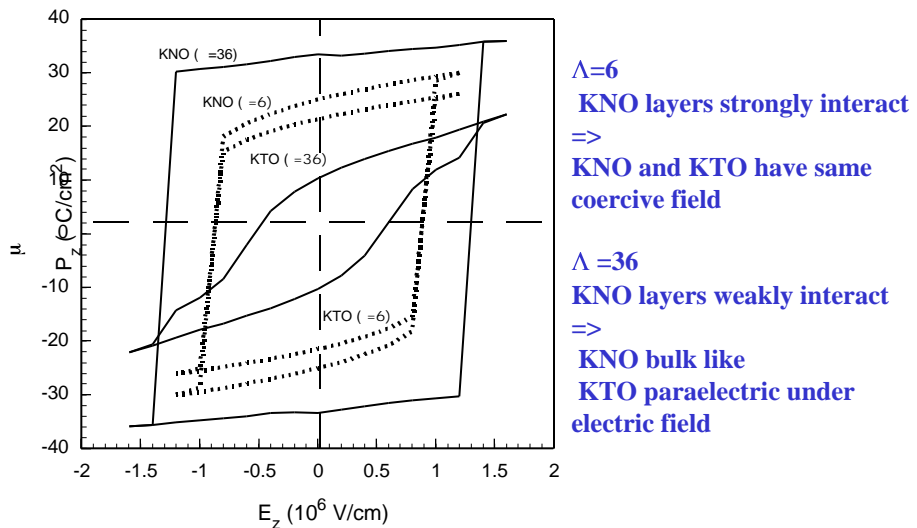
Molecular Dynamic Simulation of $\text{KNbO}_3/\text{KTaO}_3$ Superlattice Polarization on KTaO_3 Substrate



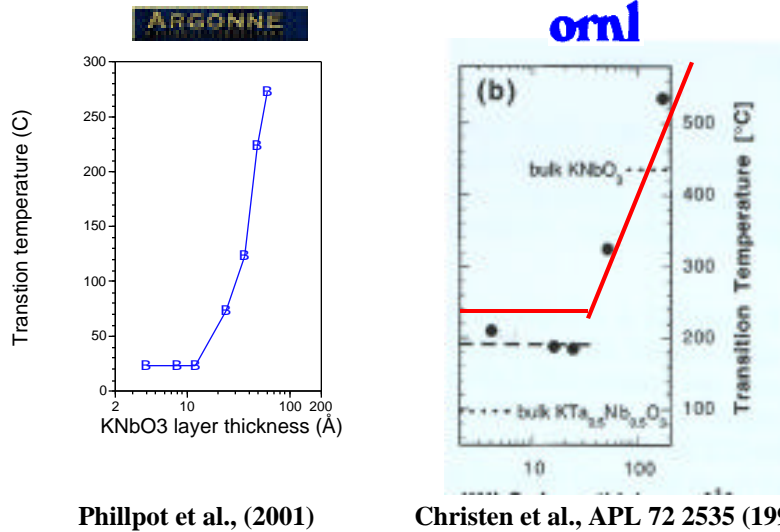
Sepliarsky et al., Phys. Rev. B, Rapid Comm. July 2001



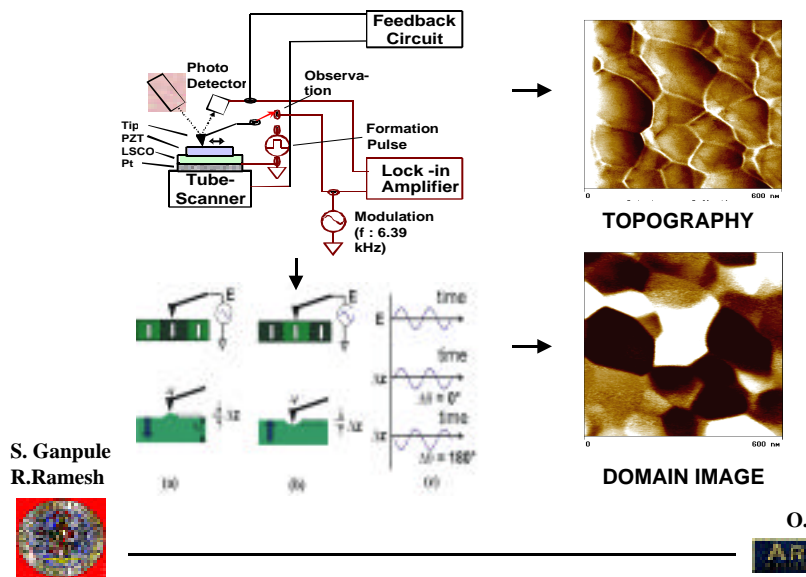
Switching Behavior of KNO/KTO Superlattices



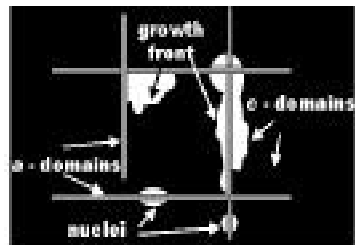
Comparison between Simulation and Experiment for Transition Temperature vs. KNO Layer Thickness



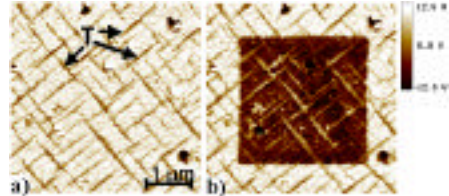
Imaging and Manipulation of Domain Behavior at the Nanoscale Using AFM Piezoresponse Imaging



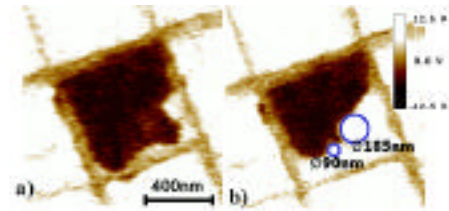
Direct Imaging of Polarization Relaxation in Ferroelectric Thin Films



Schematic illustration of the **c/a** domain architecture in ferroelectric thin films and the role of interfaces as nucleation sites



(a) AFM piezoresponse imaging of an as-deposited PZT film showing **c/a** domain structure; (b) 3 $\mu\text{m} \times 3 \mu\text{m}$ PZT film area selectively poled in the opposite, stable direction by -10 V



Piezoresponse imaging acquired during polarization relaxation of a PZT film showing the role of interfaces as domain nucleation sites (a) and pinning and bowing of 180° domains (b)



U of Maryland



Scanning probe structural study of $\text{SrBi}_2\text{Nb}_2\text{O}_9$ growth as a function of substrate miscut angle

Grow One Orientation of (103) $\text{SrBi}_2\text{Nb}_2\text{O}_9$ *
On (111) SrTiO_3

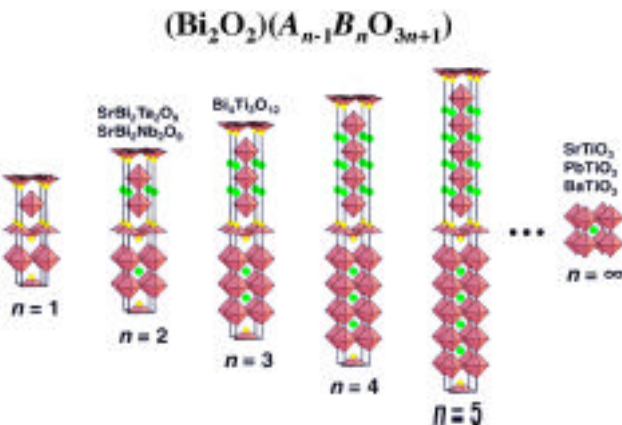
Use AFM Techniques to Study Structure & Properties of (103) $\text{SrBi}_2\text{Nb}_2\text{O}_9$ as a function of orientation

*** Advantageous fatigue resistance**

M. E. Hawley

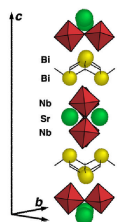


Aurivillius Homologous Series



SPM

SrBi₂Nb₂O₉ Crystal Structure

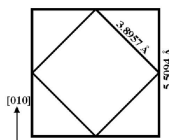


Orthorhombic: $A2_1am$

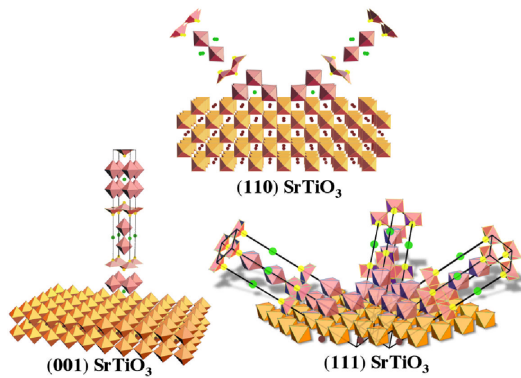
$a = 5.5094 \text{ \AA}$

$b = 5.5094 \text{ \AA}$

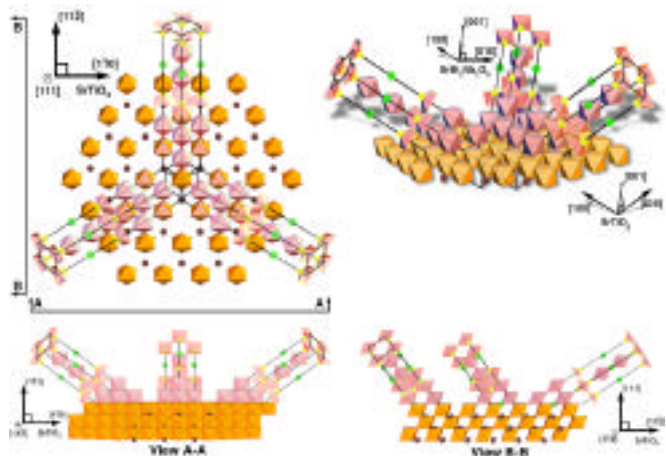
$c = 25.098 \text{ \AA}$



SrBi₂Nb₂O₉ Film Orientations On SrTiO₃ Substrates



(103) SrBi₂Nb₂O₉ / (111) SrTiO₃

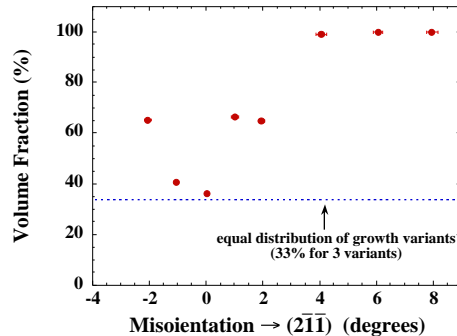


 **Los Alamos**
NATIONAL LABORATORY

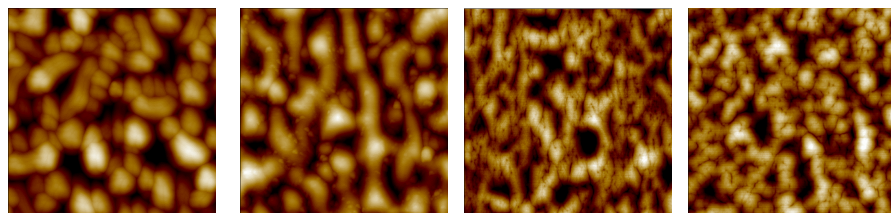
 SPIN

Scanning probe structural study of $\text{SrBiNb}_2\text{O}_9$ growth as a function of substrate miscut angle

Volume Fraction of Dominant Orientation



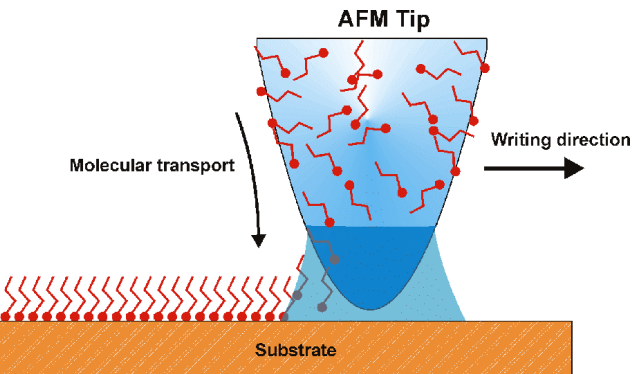
$2.5\mu - 0^\circ$ Miscut Angle $2.5\mu - 2^\circ$ Miscut Angle $2.5\mu - 4^\circ$ Miscut Angle $2.5\mu - 6^\circ$ Miscut Angle



Miscut -2 -1 0 1 2 4 6 4

RMS 20.4 22.4 21.3 20.1 24.1 5.6 5.4 5.6
(nm)

Dip-Pen nanolithography for fabrication of nanocapacitors



M. Su. L. Fu
V.P. Dravid

R. Piner, J. Zhu, F. Xu, S. Hong, C. A. Mirkin, *Science* **283**, 661 (1999)



ARGONNE

Direct sol-derived DPN patterning

(BaTiO₃ and PZT ferroelectric nanopatterns)

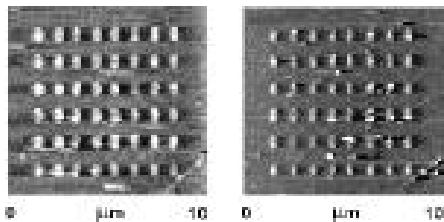


M. Su. L. Fu and V.P. Dravid
To-be-published, 2002



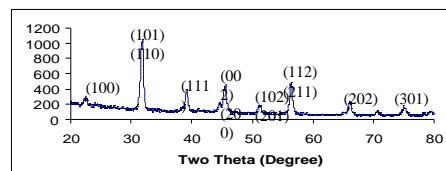
ARGONNE

Direct sol-derived DPN patterning (BaTiO₃ and PZT ferroelectric nanopatterns)



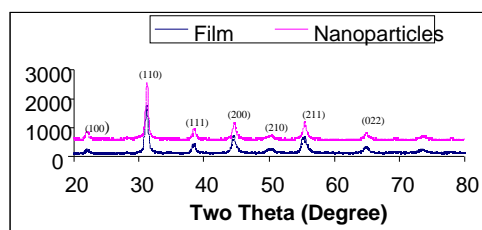
AFM image: Bar pattern before annealing
Dots ~ 100x150 nm

Bar pattern after annealing
Dots ~ 80x120 nm



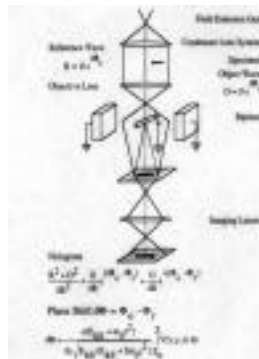
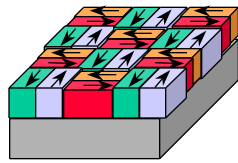
ARGONNE

Nanodot Arrays of PZT on gold substrate



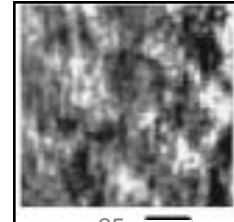
ARGONNE

Nanodot Arrays of PZT on gold substrate



Electron Holography of Charged “Nanodomains” in FE Thin Films

NSOM of BST



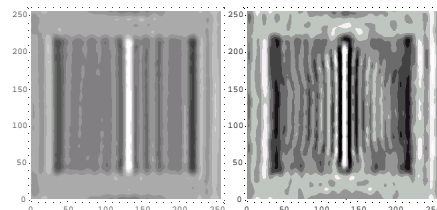
P < 0 P > 0
* C. Hubert, and J. Levy. *APL* 73, 22 (1998).

Charged nanodomains induce spatially varying electrostatic potential

→ “Phase” image in electron holography can capture e-potential – thus charge variation

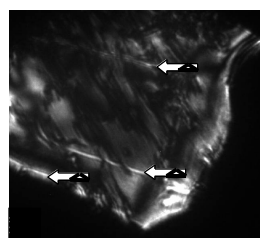


Experimental Imaging and Simulation of 180° Domain Boundaries



Simulation of a 180 degree domain boundary

Note: “White line” contrast at domain junction



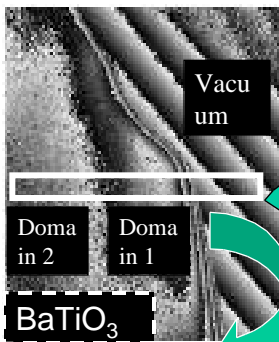
Experimental Image of 180 degree domain boundaries in BaTiO3

Note: Similar white-line contrast as in simulations



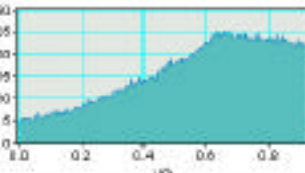
Raw/Unprocessed Holographic phase distribution across BaTiO₃ domains

(A)



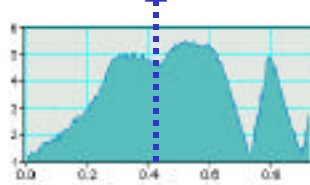
180 degree domain boundaries (A) manifest themselves as abrupt change in phase profile (C), distinct from thickness or other amplitude-contrast effects (B)

(B)



Domain Boundary

(C)



OUTLINE

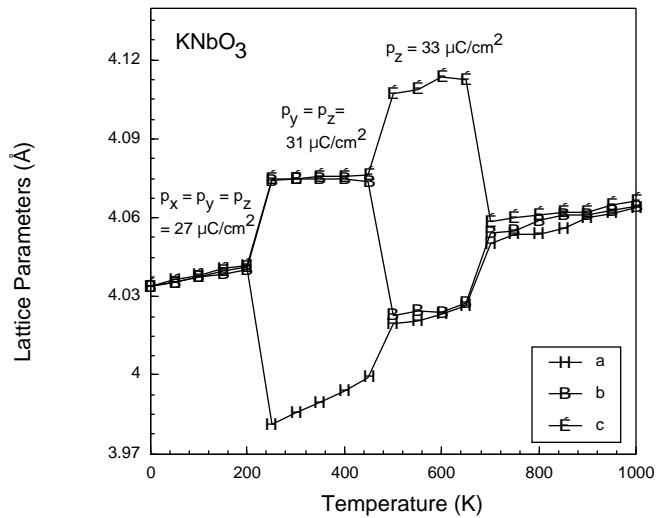
Introduction: Ferroelectricity in perovskites

- Atomic-level potentials for KNbO₃ and KTaO₃
- Polarization Reversal in KNbO₃
- *Ferroelectricity in KTa_{1-x}Nb_xO₃ solid solutions*
- *Ferroelectricity in KNbO₃/KTaO₃ superlattices*

S. R. Phillpot

Argonne

Phase diagram of KNbO₃ correctly reproduced

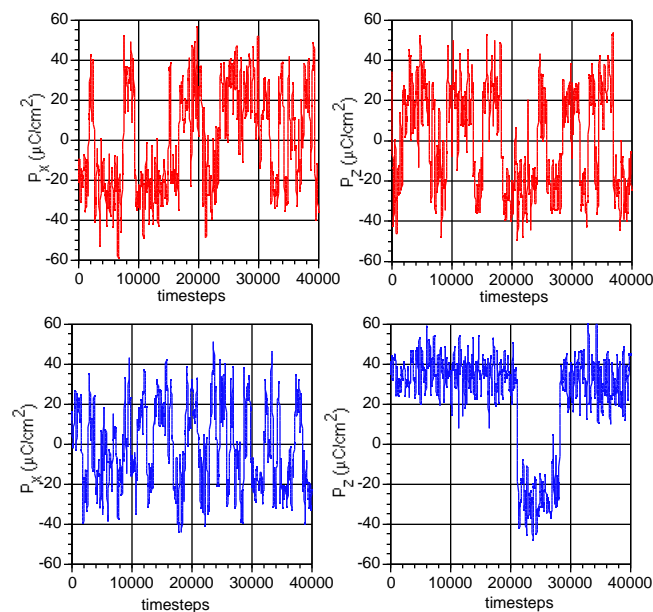


Sepliarsky et al., APL, 76, 2986 (2000)



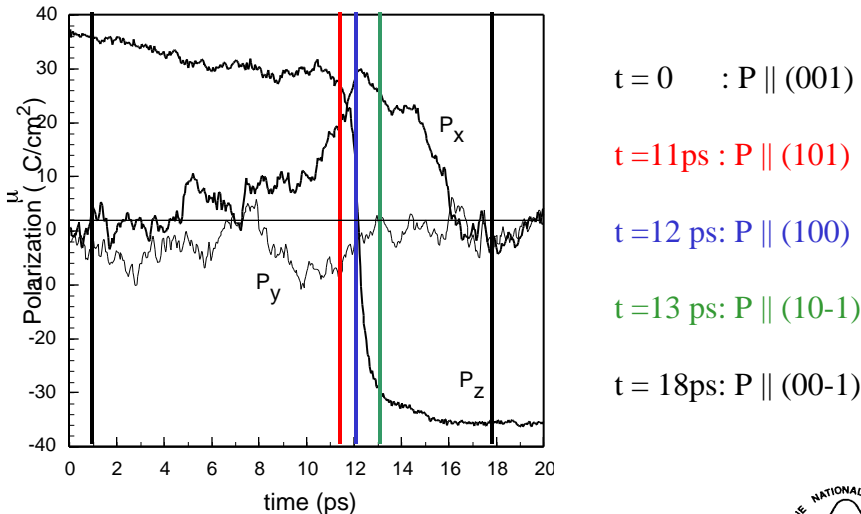
Cubic to tetragonal phase transition is order-disorder

Cubic phase
T=600K

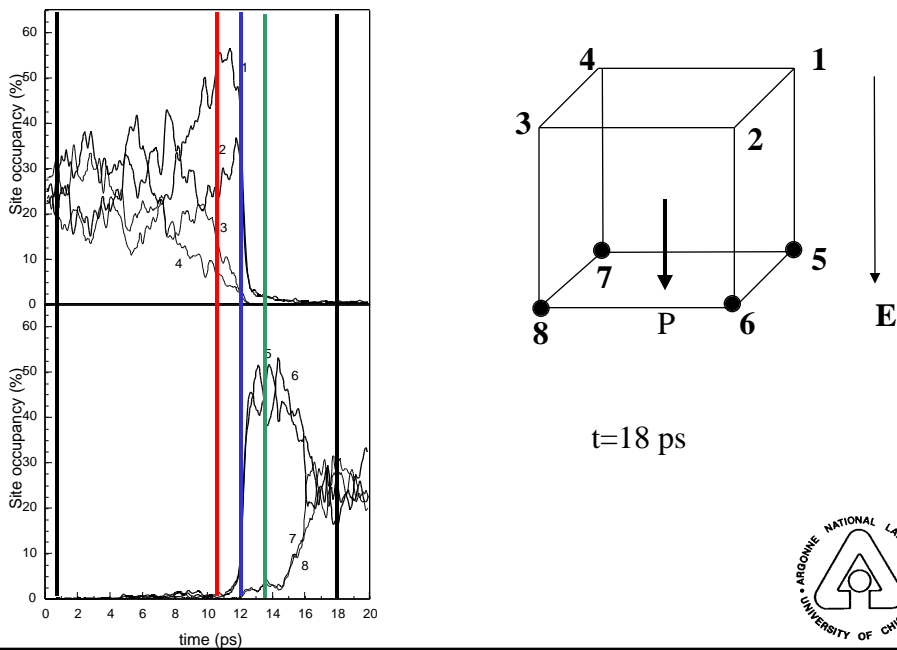


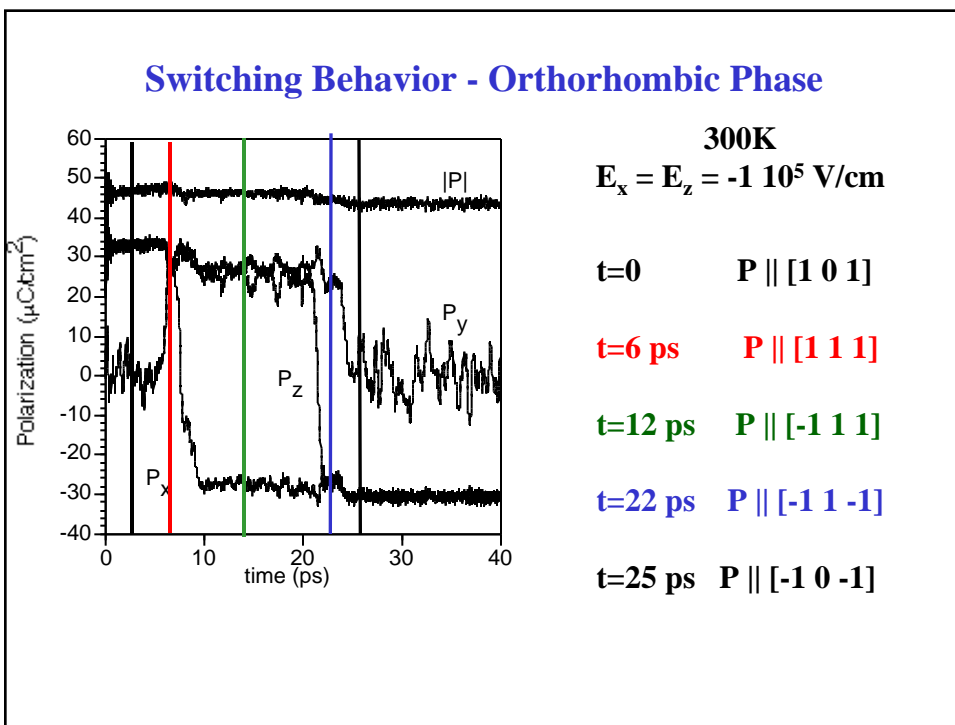
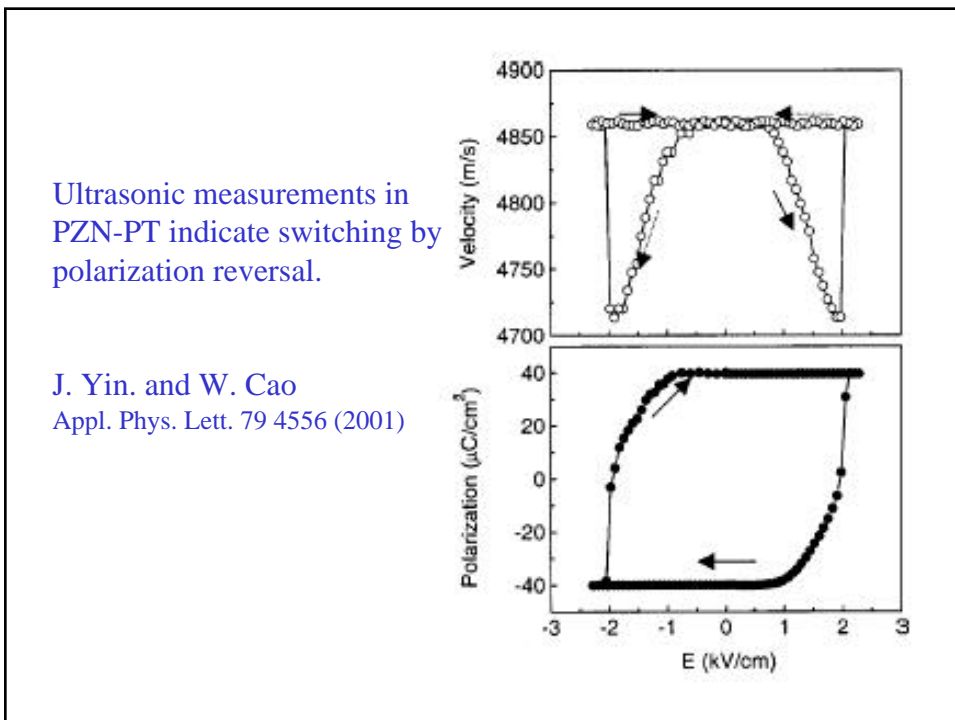
Tetragonal phase
T=800K

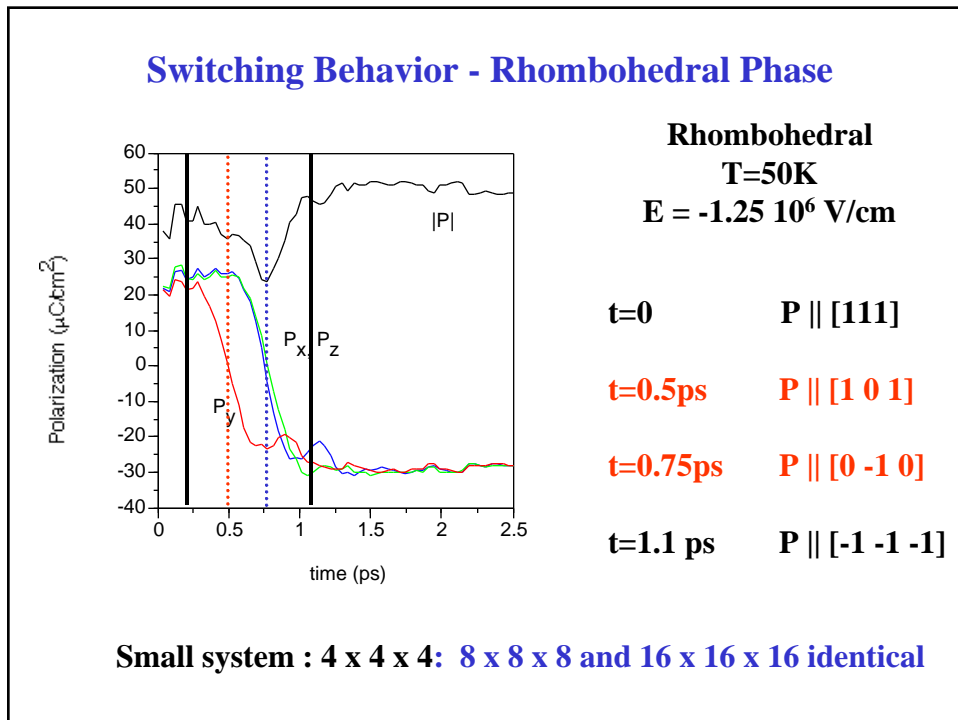
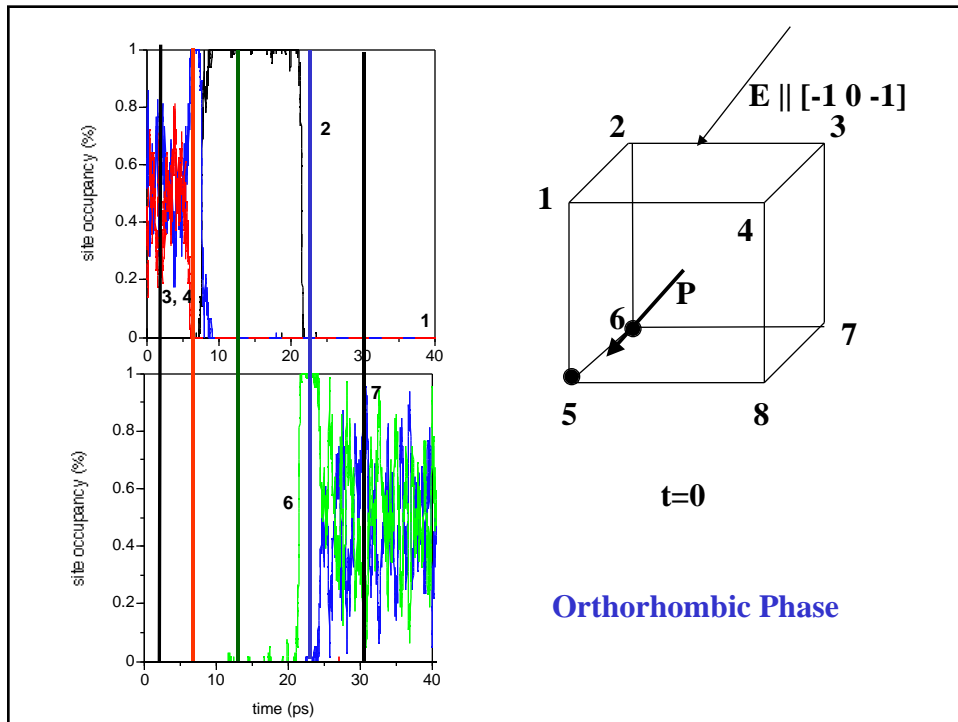
Switching behavior - Tetragonal Phase



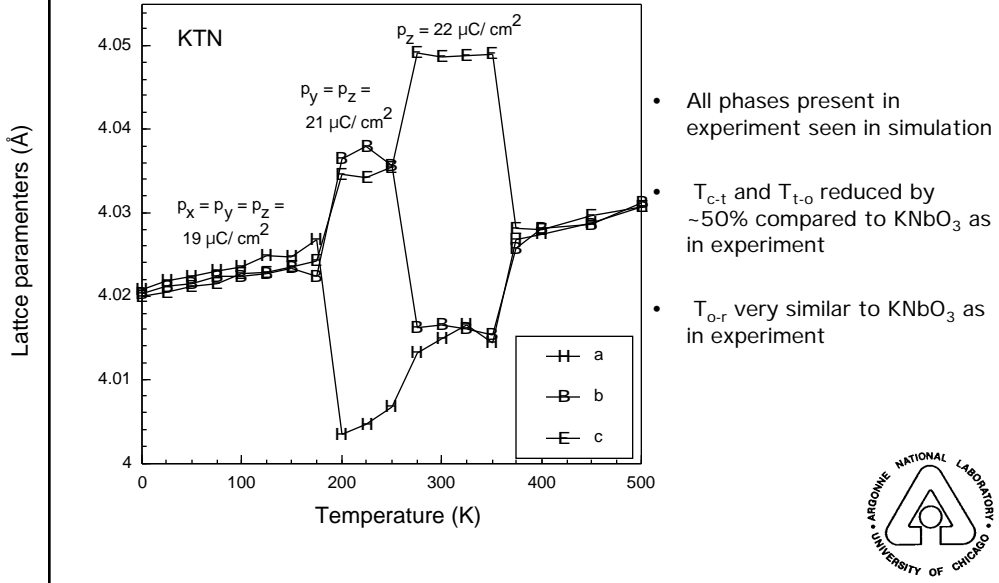
ORDER-DISORDER BEHAVIOR



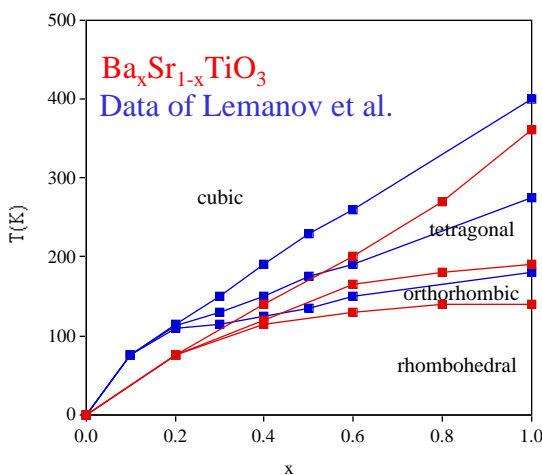




Phase diagram of KTN



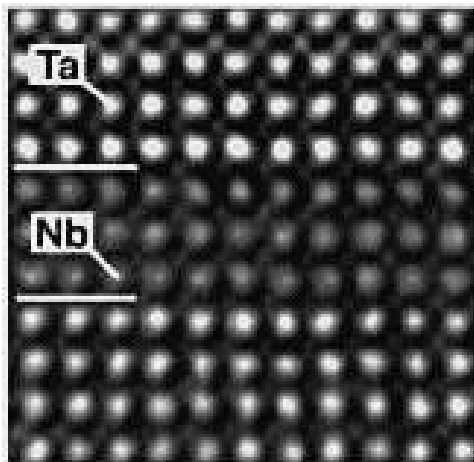
Stability diagram for Ba_xSr_{1-x}TiO₃



V. V. Lemanov et al., Phys. Rev. B 54 3151 (1996)



KNbO₃/KTaO₃ SUPERLATTICES

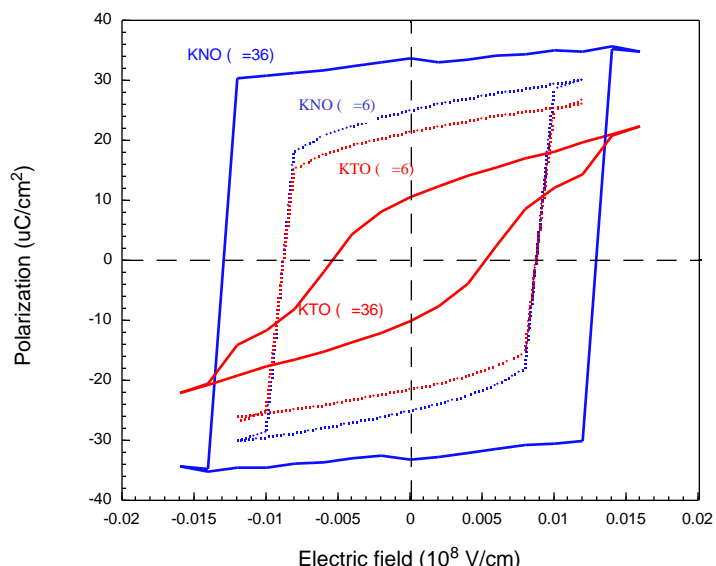


- Epitaxial KTaO₃/KNbO₃ superlattices
- grown in [001] orientation on KTaO₃
- Small lattice mismatch between KTaO₃ and KNbO₃ leads to coherent interfaces

H. M. Christen et al., APL, 72 2535 (1998)



Hysteresis Loops for Superlattice



Scientific and Technological Payoff

- New understanding in how to precisely control fabrication of perovskite films (important class of complex oxides)
- Improved understanding of the relationship between processing, structure and properties - critical for advancing perovskite-based technologies
- New understanding of ferroelectric properties (domain dynamics) at the nanoscale
- Potential for opening new avenues in nanoscience and nanotechnology

Management Plan

- Center coordinators
 - Orlando Auciello - ANL
 - Duane Dimos - SNL
- Funding - \$300K / Year
 - Three post docs and six students
 - Post docs/Students to work on collaborative projects
 - \$20K - annual workshop
- Conference calls - Videoconferencing - Website
- Annual workshop to recalibrate priorities/budget

Budget Status

Institution	Funding (\$1,000's)	Type of Support	Task/Project
ANL	\$ 45 \$ 50 \$ 20	Postdoc(Aug 01) (APS) Postdoc (hired) (Theory) Workshop (May 02) + Travel	Task 1, 2
SNL	\$ 25	Student (hired)	Task 1, 2
ORNL	\$ 50 \$ 30	Postdoc (McKee) Student (Boatner)	Task 1
LANL	\$ 25	Student	Task 2
NW	\$ 35	Student (hired)	Task 2
U of Florida	\$ 10	Partime Student	Task 1
U of Maryland	\$ 10	Partime Student	Task 1, 2
All			
TOTAL	\$300		

Publications

1. C. Thompson, G. B. Stephenson, J. A. Eastman, S. K. Streiffer, K. Ghosh, O. Auciello, G. Bai, A. Munkholm, Q. Gan, C. B. Eom, Microscopic Structural Response of Ferroelectric Domains in Epitaxial Films of $\text{Pb}(\text{Zr},\text{Ti})\text{O}_3$: Static and Dynamic Results, Advance Photon Source - User Activity Report, Vol. 1 (2001), ANL-00-5
2. C. Thompson (ANL-MSD and NIU), S. K. Streiffer, G. B. Stephenson, A. Munkholm (ANL-CHM), J. A. Eastman, O. Auciello, K. Ghosh, G. R. Bai, R. Rao (Duke Univ.), C. B. Eom (Duke Univ.), Real-Time X-Ray Interference Studies of Polarization Reversal in Ferroelectric Thin Films, Advance Photon Source - User Activity Report, Vol. 1 (2001), pp. 472, ANL-00-5
3. Carol Thompson, A. Munkholm, S.K. Streiffer, G.B. Stephenson, K. Ghosh, J.A. Eastman, O. Auciello, G.-R. Bai, M.K. Lee, and C.B. Eom, "X-Ray Scattering Evidence for the Structural Nature of Fatigue in Epitaxial $\text{Pb}(\text{Zr},\text{Ti})\text{O}_3$ Films," *Appl. Phys. Lett.* **78**, no. 22, 3511-3513 (2001)
4. A. Munkholm, S.K. Streiffer, M.V. Ramana Murty, J.A. Eastman, C. Thompson, O.Auciello, L. Thompson, J.F. Moore, and G.B. Stephenson, "Antiferrodistortive Reconstruction of the PbTiO_3 (001) Surface," *Phys. Rev. Lett.* **88**, 016101 (2001).
5. G.B. Stephenson, A. Munkholm, C. Thompson, M.V. Ramana Murty, J.A. Eastman, O. Auciello, P. Fini, S.P. DenBaars, and J.S. Speck, "Silicon Induced Layer-by-Layer Growth of GaN," *Advanced Photon Source Annual Bulletin "APS Forefront,"* October, 2001.
6. M.V. Ramana Murty, S.K. Streiffer, G.B. Stephenson, J.A. Eastman, Carol Thompson, G.-R. Bai, A. Munkholm, and O. Auciello, "In Situ X-ray Scattering Study of PbTiO_3 Chemical Vapor Deposition," *Applied Physics Letters* **80**, no. 10, 1809-1811 (2002).
7. S.K. Streiffer, J.A. Eastman, D.D. Fong, Carol Thompson, A. Munkholm, M.V. Ramana Murty, O. Auciello, G.-R. Bai, and G.B. Stephenson, , "Observation of Nanoscale 180° Stripe Domains in Ferroelectric PbTiO_3 Thin Films," accepted for publication in *Phys. Rev. Lett.* (2002).

Presentations (incomplete list)

J.A. Eastman, G.B. Stephenson, Carol Thompson, S.K. Streiffer¹, O. Auciello, M.E.M. Aanerud, L.J. Thompson, and G.-R. Bai,
 "IN-SITU X-RAY DIFFRACTION STUDIES OF FERROELECTRIC 180° STRIPE DOMAIN FORMATION IN
 HETEROEPITAXIAL PbTiO_3 THIN FILMS" at 2001 MRS Fall Meeting Symposium C: Ferroelectric Thin Films X

ARGONNE

Publications

1. Pearson, S. J., Abernathy, C. R., Overberg, M. E., Thaler, G. T., Norton, D. P., Theodoropoulou, N., Hebard, A. F., Park, Y. D., Ren, F., Kim, J., and Boatner, L. A., Wide Bandgap Ferromagnetic Semiconductors and Oxides, Journal of Applied Physics, in press (2002)
2. Norton, D. P., Kim, K. Christen, D. K., Budai, J. D., Sales, B. C., Chisholm, M. F., Kroeger, D. M., Goyal, A., and Cantoni, C., $(La,Sr)TiO_3$ as a conductive buffer for RABiTS coated conductors, Physica C, in press (2002).
3. Sigman, J., Norton, D. P., Christen, H. M., Fleming, P. H. and Boatner, L. A., Antiferroelectric behavior in symmetric $KNbO_3/KTaO_3$ superlattices, Physical Review Letters, Volume 88, Number 9, p. 097601-1, 2002.
4. Norton, D.P. ; Pearson, S.J.; Christen, H.M.; Budai, J.D., Hydrogen-assisted pulsed-laser deposition of epitaxial CeO_2 films on (001)InP, Applied Physics Letters, Volume 80, Issue 1, 2002, Pages 106-108.

Presentations

1. "Epitaxy of complex oxides on dissimilar substrates", Florida Chapter of the American Vacuum Society, AVS-FSM Joint Symposium, Orlando, FL, March 2002.
2. "Current status of coated conductor development based on the RABiTS Process," 5th European Conference on Applied Superconductivity, Copenhagen, Denmark, August 2001
3. "Reactive sputter deposition of epitaxial CeO_2 on (001) Ge and InP," MRS Workshop on Dielectric Science & New Functionality in Device Physics for Crystalline Oxides on Semiconductors, Chattanooga, TN, September 2001.
4. "Heteroepitaxial growth of complex oxides on metals and semiconductors," 2001 Spring Meeting of the Materials Research Society, San Francisco, CA, April 2001.
5. "Nanostructured oxide interfaces and thin films," International Conference on Metallurgical Coatings and Thins Films, San Diego, CA, May 2001.



ornl

Publications

1. J. Sigman, H. M. Christen, P. H. Fleming, L. A. Boatner, and D. P. Norton, "Evidence for Antiferroelectric Behavior in $KNbO_3/KTaO$ Superlattices," Materials Research Society Symposium Proceedings 720, (2002) (submitted for publication).

Presentations

1. L. A. Boatner, "Potassium Tantalate and KTN – Substrates for the Growth of Epitaxial Ferroelectric Films and Superlattices," Presented at the Ferroelectrics Workshop-Puerto Rico, (FWPR-01), San Juan, Puerto Rico, June 1-2, 2001.
2. David Norton, J. Sigman, Hans Christen, Pam Fleming, Lynn Boatner, and Mark Reeves, "Evidence for Antiferroelectric Behavior in $KNbO_3/KTaO_3$ Superlattices," Presented at the 2002 Spring MRS Meeting, San Francisco, CA April 1-5, 2002.



ornl

Publications

1. B.T. Liu, K. Maki, Y. So, V. Nagarajan, R. Ramesh, J. Lettieri, J.H. Haeni, D.G. Schlom, W. Tian, X.Q. Pan, F.J. Walker and R.A. McKee, "Epitaxial La-doped SrTiO₃ on silicon: A conductive template for epitaxial ferroelectrics on silicon", *Appl. Phys. Lett.*, in press (2002).
2. R.A. McKee, F.J. Walker and M.F. Chisholm, "Physical Structure and Inversion Charge at a Semiconductor Interface with a Crystalline Oxide", *Science* **293**, 468(2001).
3. A.Lin, X. Hong, V.Wood, A.A. Verevkin, C.H. Ahn, R.A. McKee, F.J. Walker and E.D. Specht "Epitaxial Growth of Pb(Zr_{0.2}Ti_{0.8})O₃ on Si and its Nanoscale Piezoelectric Properties", *Appl Phys Lett* **78**, 2034(2001).

Invited Presentations

1. Interfacial Structure of Crystalline Oxides on Semiconductors, *The American Physical Society, March 02*.
2. Crystalline Oxides on Silicon-Interface Structure and the Schottky Barrier, *International Semiconductor Device Research Symposium (ISDRS), Dec. 01*.
3. Silicide and Oxide Heteroepitaxy on Silicon-what we know and what we think, *MRS Fall Symposium, November 01*.
4. Interfacial Physics of Crystalline Oxides on Semiconductors, *The American Physical Society, March 01*.
5. Fred Walker, Methodologies and Consequences of a Layer-Sequencing Approach to Interface Physics for an Oxide/Semiconductor Structure, *Materials Research Society, Sept 01*.
6. Malcolm Stocks, First Principles Studies of the Atomistic and Electronic Structure of Crystalline Oxides on Silicon, *Materials Research Society, Sept 01*.
7. Curt Billman, Electrical Characteristics of Crystalline Alkaline Earth Oxides on Semiconductors, *Materials Research Society, Sept 01*.

ornl



Publications

1. *Long-Ranged Ferroelectric interactions in Perovskite Superlattices*, M. Sepliarsky, S. R. Phillpot, D. Wolf, M. G. Stachiotti and R. L. Migoni, *Physical Review B*, **64**, 0601010(R), (2001).
2. *Ferroelectric Properties of KNbO₃/KTaO₃ Superlattices by Atomic-Level Simulation*, M. Sepliarsky, S. R. Phillpot, D. Wolf, M. G. Stachiotti and R. L. Migoni, *Journal of Applied Physics* **90**, 4509-4519 (2001).
3. *Dynamics of Polarization Reversal in a Perovskite Ferroelectric by Molecular-Dynamics Simulation*, M. Sepliarsky, S. R. Phillpot, S. K. Streiffer, M. G. Stachiotti and R. L. Migoni, *Applied Physics Letters* **79**, 4417-4419 (2001).
4. *Phase Transitions and Dynamical Behavior in KNbO₃/KTaO₃ Superlattices by Molecular-Dynamics Simulation*, M. Sepliarsky, S. R. Phillpot, M. G. Stachiotti and R. L. Migoni, *Journal of Applied Physics* **91**, 3165-3171 (2002).
5. *Order-Disorder Behavior in KNbO₃ and KNbO₃/KTaO₃ Solid Solutions and Superlattices by Molecular-Dynamics Simulations*, S. R. Phillpot, M. Sepliarsky, S. K. Streiffer, M. G. Stachiotti and R. L. Migoni, *Proceedings of the Conference on Fundamental Physics of Ferroelectric 2002*, to be published as an AIP Proceedings volume.

Presentations

1. M. Sepliarsky, S. R. Phillpot, M. G. Stachiotti and R. L. Migoni, *Dynamical Behavior in Perovskite Ferroelectrics*, Invited Talk in Symposium D, Fall MRS Meeting, Boston MA, 26 November 2001.
2. M. Sepliarsky, S. R. Phillpot, M. G. Stachiotti and R. L. Migoni, *Phase Transitions and Dynamical Behavior in a Perovskite Ferroelectric*, Invited Talk at TMS Annual Meeting, Seattle WA, 18 February 2002.
3. M. Sepliarsky, S. R. Phillpot, M. G. Stachiotti and R. L. Migoni, *Switching Dynamics in Ferroelectric Perovskites*, Invited Talk at American Ceramic Society Meeting, St. Louis, MO, April 30 2002.

ARGONNE